UNUSUAL METALLOPORPHYRIN COMPLEXES OF RHENIUM AND TECHNETIUM

M. Tsutsui, et al

Texas A and M University

Prepared for:

Office of Naval Research

6 June 1975

OFFICE OF NAVAL RESEARCH

Contract N00014-68-A-0308-0006

Task No. NR 356-559

TECHNICAL REPORT NO. 10

Unusual Metalloporphyrin Complexes of Rhenium and Technetium[1]

by

M. Tsutsui, C. P. Hrung, D. Ostfeld, T. S. Srivastava,
D. L. Cullen and E. F. Meyer, Jr.

Prepared for Publication

in the

Journal of the American Chemical Society

Texas A&M University
Department of Chemistry
College Station, Texas

June 6, 1975

DOCUMENT CONTROL DATA - R & D

(Security classification of title, body of abstract and indexing annotation must be entered when the overall report is classified)

1. ORIGINATING ACTIVITY (Corporate author) Department of Chemistry Texas A&M University College Station, Texas 77843	2a. REPORT SECURITY CLASSIFICATION none 2b. GROUP

3. REPORT TITLE

Unusual Metalloporphyrin Complexes of Rhenium and Technetium[1]

4. DESCRIPTIVE NOTES (Type of report and inclusive dates)
Technical Report

5. AUTHOR(S) (First name, middle initial, last name)

Minoru Tsutsui, Chang-Po Hrung, David Ostfeld, T. S. Srivastava, David L. Cullen
Edgar F. Meyer, Jr.

6. REPORT DATE June 6, 1975	7a. TOTAL NO. OF PAGES 51 61	7b. NO. OF REFS 76
8a. CONTRACT OR GRANT NO. N00014-68-A-0308-0006 b. PROJECT NO. 987 c. d.	9a. ORIGINATOR'S REPORT NUMBER(S) Technical Report No. 10 9b. OTHER REPORT NO(S) (Any other numbers that may be assigned this report)	

10. DISTRIBUTION STATEMENT

Approved for public release; distribution unlimited.

11. SUPPLEMENTARY NOTES In press, Accepted for publication in Journal of the American Chemical Society	12. SPONSORING MILITARY ACTIVITY Office of Naval Research, Department of the Navy Arlington, Virginia 22217

13. ABSTRACT

Both the rhenium and technetium homodinuclear porphyrins are centrosymmetric complexes having two metals bonded to the porphyrin, one above and one below the plane of the macrocycle while the porphyrin macrocycle is highly distorted. The metal ions are not positioned directly over the center of the macrocycle, but are set to one side such that each metal ion is bonded to three nitrogen atoms. There is a small but significant difference in the metal-metal distance, with the Tc-Tc distance being 0.02 Å shorter. The M-M distance (3.101 Å for the Tc complex) though somewhat long for bonding is short enough that some metal-metal interaction may be possible. Due to the observed similarity in both their chemical and physical properties, it was assumed that not only the homo- and heterodinuclear metalloporphyrins but also the monometallic porphyrin complexes of Re and Tc have similar structures. A fluxional character of both Re and Tc monometallic porphyrin complexes was observed by variable-temperature pmr spectral studies. This fluxional phenomenon is best explained by the intramolecular rearrangement of the metal-carbonyl group among the four ring nitrogen atoms of porphyrin and a concomitant movement of the N-H proton. A novel thermal disproportionation of H-MP)$Tc(CO)_3$ to MP-$[Tc(CO)_3]_2$ and H_2MPIXDME was also observed.

DD FORM 1 NOV 68 1473

Security Classification

Security Classificat.

14. KEY WORDS	LINK A		LINK B		LINK C	
	ROLE	WT	ROLE	WT	ROLE	WT
unusual metalloporphyrin complexes of rhenium						
unusual metalloporphyrin complexes of technetium						
$TPP[Re(CO)_3]_2$						
$TPP[Tc(CO)_3]_2$						
centrosymmetric complexes						
$(H\text{-}TPP)Re(CO)_3$						
fluxional character						
$(H\text{-}MP)Tc(CO)_3$						
semiconductors						
superconductors						
catalysts						

Unusual Metalloporphyrin Complexes of Rhenium and Technetium[1]

M. Tsutsui*, C. P. Hrung, D. Ostfeld[2] and T. S. Srivastava
Contribution from the Department of Chemistry,
Texas A&M University, College Station, Texas 77843

D. L. Cullen and E. F. Meyer, Jr.
Contribution from the Department of Biochemistry and Biophysics,
Texas Agricultural Experiment Station,
Texas A&M University, College Station, Texas 77843

Abstract:

By reaction of dirhenium decacarbonyl, $Re_2(CO)_{10}$, or ditechnetium decacarbonyl, $Tc_2(CO)_{10}$, with mesoporphyrin IX dimethyl ester, H_2MPIXDME, or meso-tetraphenylporphine, H_2TPP, monometallic and bimetallic porphyrin complexes of rhenium and technetium were synthesized. Visible spectroscopy indicates that first the monometallic and then the bimetallic porphyrin complex is formed. The monometallic complex of rhenium can further react with either $Re_2(CO)_{10}$ or $Tc_2(CO)_{10}$ to form the homo- and heterodinuclear metalloporphyrin complexes. Structural data for the homodinuclear metalloporphyrin complexes of both rhenium and technetium, TPP$[Re(CO)_3]_2$ and TPP$[Tc(CO)_3]_2$, were obtained by single crystal X-ray diffraction.

Both the rhenium and technetium homodinuclear porphyrins are centrosymmetric complexes having two metals bonded to the porphyrin, one above and one below the plane of the macrocycle while the porphyrin macrocycle is highly distorted. The metal ions are not positioned directly over the center of the macrocycle, but are set to one side such that each metal ion is bonded to three nitrogen atoms. There is a small but significant difference in the metal-metal distance, with the Tc-Tc distance being 0.02 Å shorter. The M-M distance (3.101 Å for the Tc complex) though some-

what long for bonding is short enough that some metal-metal interaction may be possible. Due to the observed similarity in both their chemical and physical properties, it was assumed that not only the homo- and heterodinuclear metalloporphyrins but also the monometallic porphyrin complexes of Re and Tc have similar structures. Proton magnetic resonance spectrum of (H-TPP)$Re(CO)_3$ gave evidence for the proposed structure of the monometallic porphyrin complexes. In the monometallic complexes, the porphyrin acts as a tridentate instead of a tetradentate ligand, while in the bimetallic complexes, the porphyrin acts as a hexadentate ligand; both of these are considered non-classical coordination numbers for the porphyrin ligand. A fluxional character of both Re and Tc monometallic porphyrin complexes was observed by variable-temperature pmr spectral studies. This fluxional phenomenon is best explained by the intramolecular rearrangement of the metal-carbonyl group among the four ring nitrogen atoms of porphyrin and a concomitant movement of the N-H proton. A novel thermal disproportionation of (H-MP)$Tc(CO)_3$ to MP-$[Tc(CO)_3]_2$ and H_2MPIXDME was also observed. A dissociation and recombination of the metal-carbonyl moieties and the porphyrin ligands between two of the (H-MP)$Tc(CO)_3$ molecules would seem interpretable for this unusual coordination phenomenon.

****

Introduction

There is a growing interest in metalloporphyrins because of the unique nature of the coordination chemistry of these materials[3-8] and also because of their obvious relevance as biological models[9-12] (such as chlorophyll[13], hemoglobin[14], cytochrome[15], and vitamin B_{12}[16,17]). Changes or modification of general porphyrin metabolism are associated with cancer, drug metabolism, and specific disease syndromes.[18] Thus, the biological functions of metalloporphyrins are of a great deal of importance. Most of the research in metalloporphyrins not only stems from interest in the biological systems to which they are related, but also stems from the search for new semiconductors[19], superconductors[20], anticancer drugs[21], tumor localization agents[22], and catalysts[23]. Even without their biological and industrial implications the properties and a large variety of structural types[4] of metalloporphyrins would be studied for their purely theoretical importance.

Understanding of the porphyrin system has advanced appreciably in recent years.[8] Except for lanthanides[24] and actinides, almost every metal in the periodic table has been coordinated to a porphyrin.[7] Any reasonable porphyrin complex desired by inorganic chemists seems attainable through the powerful synthetic methods which are now available. These methods included: (1) reaction of a porphyrin with a metallic salt (acetate, halide, oxide, etc.) in an acidic or basic medium[3]; (2) supplying the metal in the form of carbonyls[25,26], carbonyl halides[27,28], or other organometallic compounds[26,29]; (3) the use of an acetylacetonate complex[24,30] as a source of metal; (4) reaction in a medium of high dielectric constant (such as

phenol, benzonitrile, N,N -dimethylformamide, etc.)[31,32].

The major problem in the traditional metalloporphyrin syntheses is that of the difficulty in dissolving both the free porphyrin and the metallic salt simultaneously into the same solution under reactive conditions.[3] This is due to the fact that good solvents for the porphyrins in their unionized forms are generally poor solvents for simple metallic ions and vice versa. In an acidic medium, the porphyrin exists mostly in the unreactive protonated form. In a basic medium, on the other hand, the porphyrin must compete (often disadvantageously) with the solvent as a complexing agent for the metal ion. The solubility problem was overcome by using high dielectric solvents which are capable of dissolving both the free porphyrin and the metallic salt. It is general, rapid, and convenient; gives high and large yields; and requires no special reagents. This method was developed by Adler[31] and further extended by Buchler[32] for the preparation of a number of previously unknown metalloporphyrin complexes of scandium[30], zirconium[30], hafnium[32], niobium[32], tantalum[32], tungsten[33], rhenium[33], and osmium.[34] These new metalloporphyrins have been used to demonstrate the geometric limits of the porphyrin ligand[32] as well as some additional geometries which it can assume.[35] It is of interest that metal acetylacetonates are found both readily available and reasonably soluble in non-polar organic solvents, and are therefore used as useful metal source for the preparation of new metalloporphyrins.[24,30,35] The solubility problem in the synthesis of metalloporphyrins was also overcome by the use of organometallic compounds as the metal source.[26,29] But the inconvenience involved in obtaining air-sensitive organometallic derivatives and the availability of other methods have prevented greater use of the organometallics as starting materials.

The use of metal carbonyls for the insertion of metal ions into porphyrins was introduced by Tsutsui[25] in 1966. This method has been found quite general for metals having suitable derivatives and developed to an useful and unique method in the syntheses of unusual metalloporphyrins within the last decade.[7] In addition to a number of previously reported metalloporphyrins, the reaction of metal carbonyls or metal carbonyl halides with neutral porphyrins has led to the syntheses of new metalloporphyrin complexes of chromium[25,36], molybdenum[36,37], ruthenium[28,38], rhodium[39-42], iridium[27,29], rhenium[43,44], and technetium[45,46]. Except for the chromium and molybdenum porphyrin complexes, carbonyl groups are retained by the metals in the new metalloporphyrins. For rhodium, rhenium, and technetium metalloporphyrins, unusual bimetallic complexes with a low oxidation state and out-of-plane structure were obtained for the first time. The unusual bimetallic rhodium complex and its derivatives were reported by Yoshida and co-workers.[40-42] More detailed spectral and structural data for the unusual monometallic and bimetallic rhenium and technetium porphyrin complexes are described and compared in this paper. Both the out-of-plane rhenium and technetium bimetallic complexes of meso-tetraphenylporphine are isostructural. The single crystal X-ray diffraction analyses data obtained for the technetium complex is superior to that obtained for the rhenium complex. Absorption effects are much smaller in the former and the metal ion contributes to a smaller percentage of the scattering power, which means the non-metal atoms can be located with much more accuracy. As a result more may be said about the structural details of the porphyrin macrocycle.

Results:

Unusual Rhenium Metalloporphyrin Complexes

Reflux of decalin solutions containing $Re_2(CO)_{10}$ and porphyrin have given several different rhenium porphyrins, depending on the ratios of reactants and on the porphyrin used. Among the compounds isolated were: (monohydrogen mesoporphyrin IX dimethyl esterato) tricarbonylrhenium(I), $HMPRe(CO)_3$, (I); (monohydrogen meso-tetraphenylporphinato)tricarbonylrhenium(I), $HTPPRe(CO)_3$, (II); μ-[mesoporphyrin IX dimethyl esterato]bis[tricarbonylrhenium(I)], $MP[Re(CO)_3]_2$ (III); μ-[meso-tetraphenylporphinato]bis[tricarbonylrhenium(I)], $TPP[Re(CO)_3]_2$, (IV).

The characterization of these compounds was done by elemental analyses, visible, infrared, proton magnetic resonance, and mass spectra (Tables 1 and 2).

Compound II was particularly appropriate for pmr studies. Its pmr spectrum in deuterochloroform showed an upfield singlet at δ - 4.0 for the N-H proton; two broad multiplets at 7.87 and 8.30 for the phenyl protons; and three sets of signals (Figure 1) for the β-pyrrole protons. The peaks due to the β protons include an AB quartet[47] centered at 9.11 (J_{AB} = 5.0 Hz, with a ratio between the outer and the inner peaks of 1:2.2); a doublet centered at 8.88 (J = 2.0 Hz), and a singlet centered at 8.72. The relative intensities of these sets of peaks were 2:1:1. This is consistent with coordination between the rhenium atom and the nitrogen atoms of three adjacent pyrroles (rings B, C, and D of Figure 2). The uncoordinated pyrrole nitrogen atom (ring A in Figure 2) would be bound to a proton. This proton would cause the splitting observed at 8.88, and was completely exchangeable with deuterium. In the deuteriated sample the doublet

centered at 8.88 collapsed to a singlet of about twice the peak height but the same area. This type of coordination was found for each metal ion in the X-ray determination of the structure of the bimetallic complex IV.[44]

Compound III was also prepared by the reaction of H_2MPIXDME with excess $Re_2(CO)_{10}$ in refluxing decalin under argon. The reaction occurred in a stepwise manner by forming complex I as reaction intermediate. This phenomenon was detected by a stepwise change of visible absorption spectra (Figure 3) and a continuous change of color in the reaction mixture (from an initial reddish purple color to greenish brown and finally to a dark reddish brown color). However, this stepwise reaction is not reversible. Attempts at the conversion of III to I by reflux in decalin with exess H_2MPIXDME were unsuccessful. The formation of these two unusual rhenium metalloporphyrin complexes is seen to proceed via the following reaction scheme, where MP represents the dianion of mesoporphyrin IX dimethyl ester:

$$H_2MP + Re_2(CO)_{10} \xrightarrow{\Delta} MP[Re(CO)_3]_2 + H_2\uparrow + 4CO\uparrow \quad (1)$$

$$2\ H_2MP + Re_2(CO)_{10} \xrightarrow{\Delta} 2\ (H\text{-}MP)Re(CO)_3 + H_2\uparrow + 4CO\uparrow \quad (2)$$

$$2\ (H\text{-}MP)Re(CO)_3 + Re_2(CO)_{10} \xrightarrow{\Delta} 2\ MP[Re(CO)_3]_2 + H_2\uparrow + 4CO\uparrow \quad (3)$$

Derivatives of Monorhenium Metalloporphyrin Complex

The reaction of I with excess $Re_2(CO)_{10}$ to form the dirhenium complex, III, suggested the possibility of making a series of complexes in which the porphyrin ring is bound to both rhenium atom and an atom of another metal. Although this could not be done with all metals, I did react further with several mono- and divalent cations of heavy metals (Ag^+, Hg^{++}, and Pb^{++}) in a basic solvent.[48] Evidence for these reactions came from changes in the visible absorption spectra of the solutions (Table 3). It is presumed that monovalent cations replace the remaining pyrrole proton of I, forming a 1:1 complex. Divalent cations are thought

to similarly replace a pyrrole proton from each of two molecules of I, forming a sandwich-type complex with the heavy metal ion situated between two porphyrin rings. The metal-nitrogen bonds thus formed are weak and the products could not be purified due to decomposition in air. Partial decomposition is also shown by the molecular weight and analytical results. It is of interest that the reaction of I with neutral copper acetate (2 : 1 mole ratio) in a basic solvent at room temperature for 5 hours results in the replacement of the rhenium-carbonyl moiety by cupric ion to form a square planar copper(II) porphyrin complex.

By reaction of I with ditechnetium decacarbonyl, $Tc_2(CO)_{10}$, in 1 to 0.6 mole ratio in refluxing decalin under argon, an unusual heterodinuclear metalloporphyrin complex, [tricarbonyltechnetium(I)]-μ-[meso-porphyrin IX dimethyl esterato][tricarbonylrhenium(I)], $(OC)_3TcMPRe(CO)_3$, (V), was prepared.[45] This new complex was also characterized by elemental analyses, molecular weight determination, visible absorption, infrared, pmr, and mass spectra. Except for small shifts, the visible absorption spectrum of V in methylene chloride resemble that of III. Because of the similarities in physical and chemical properties among III, IV and V, structures identical with that of IV were proposed for III and V as shown in Figure 4.

Fluxional Behavior

Due to its more highly symmetric porphyrin (Figure 2c), the pmr spectrum of II is much simpler than that of I. At room temperature the pmr spectrum showed the nonequivalence of the β-pyrrole protons in II (Figure 1) and also the bridged methine protons in I. Temperature dependent pmr spectral changes for I and II dissolved in 1,1,2,2-tetrachloroethane (bp 146°) are shown in Figure 5. As the temperature is raised, the peaks broaden, coalesce, and gradually sharpen. The changes have all been shown

to be completely reversible with temperature. These results illustrate that both I and II display a fluxional character.[49] This is best explained in terms of an intramolecular rearrangement of the rhenium-carbonyl group among the four ring nitrogens of porphyrin and a concomitant movement of the N-H proton. It can also be regarded as an intramolecular substitution at rhenium. A solution containing I and excess H_2MPIXDME showed no broadening of the free ligand bridged methine proton peak in the fast exchange region for I. Further, the coalescence temperatures were not shifted by changes in the concentrations of the complexes within the standard deviations of the experiment (ca $\pm$ 5°). These results show that the thermal rearrangement process is intramolecular rather than intermolecular. Also, the occurence of either dissociation and recombination of the metal-carbonyl moiety and the porphyrin ligand or interchange of ligands between two molecules at high temperature is ruled out by the failure of attempts to convert III to I by reflux in decalin with excess porphyrin.

Unusual Technetium Metalloporphyrin Complexes

By reflux of $Tc_2(CO)_{10}$ and porphyrin in decalin, in a manner similar to that used in preparing the rhenium complexes, several technetium porphyrins were prepared. Depending on the porphyrin used and the ratios of reactants, the following compounds were prepared: (monohydrogen mesoporphyrin IX dimethyl esterato)tricarbonyltechnetium(I), $HMPTc(CO)_3$, (VI); μ-[mesoporphyrin IX dimethyl esterato]bis[tricarbonyltechnetium(I)], $MP[Tc(CO)_3]_2$, (VII); and μ-[meso-tetraphenylporphinato]bis[tricarbonyltechnetium(I)], $TPP[Tc(CO)_3]_2$, (VIII).

These compounds are considered to be structurally similar to the corresponding rhenium complexes. A single crystal X-ray diffraction analysis of VIII, reported here, has confirmed the similarity.

The reaction of H_2MPIXDME and $Tc_2(CO)_{10}$ in a mole ratio of 1 to 0.6 was used to give the monotechnetium complex, VI. However, when the same reaction was run for longer periods of time; the products were the free porphyrin and μ-[mesoporphyrin IX dimethyl esterato]bis[tricarbonyl-technetium(I)], $MP[Tc(CO)_3]_2$, (VII). The results of these two reactions suggest that H_2MPIXDME and $Tc_2(CO)_{10}$ react initially to form $(H\text{-}MP)Tc(CO)_3$ which then disproportionates (Figure 6) into $MP[Tc(CO)_3]_2$ and H_2MPIXDME. This behavior was confirmed by heating a benzene/dichloromethane (50/50) solution of a purified sample of VI to dryness in a hot water bath at 50-60°. Chromatography on a talc column showed the presence of both H_2MPIXDME and VII.

Complex VII was stable at room temperature but it was thermally unstable in refluxing decalin in a different manner than complex VI. When a decalin solution of VII was refluxed under argon for more than four hours, a large amount of solid material precipitated from the decalin. The unknown solid compound, (IX), was insoluble in most organic solvents but was slightly soluble in methylene chloride. The visible spectrum of the solution had a sharp absorption at 358 nm and three weak, broad peaks at 397 (Soret), 500, and 540 nm. The unknown compound turned black above 260° without melting. The infrared spectrum of IX in the solid phase (KBr) also showed two strong metal-carbonyl stretches at 2044 and 1925 cm^{-1} and a split ester carbonyl peak centered at 1725 cm^{-1}. A similar splitting of an ester carbonyl peak has been observed in the solid ruthenium metalloporphyrin complex, MPRuCO, and tentatively assigned to coordination

between the ester carbonyl and the metal.[50] The unknown solid, IX, may be a coordination polymer[51,52] involving similar coordination between a metal and an ester carbonyl.

The elemental analyses results and all of the spectra data for both rhenium and technetium metalloporphyrin complexes, I-IX, are summarized in Tables 1 and 2.

X-Ray Structural Data

A preliminary study on the single crystal X-ray diffraction analysis of $TPP[Re(CO)_3]_2$, IV, has already been reported.[44] This structure has now been fully refined. In addition, the structure of the analogous technetium complex $TPP[Tc(CO)_3]_2$, VIII, has been determined and is reported here. Results of the analyses are tabulated in Tables 4-10. Within standard deviations the two compounds are virtually isostructural. Both are centrosymmetric complexes having two metal ions bonded to the porphyrin, one above and one below the plane of the macrocyclic ligand. A comparison of these two complexes of Group VIIb congeners is of interest.

The X-ray data obtained for the technetium complex is superior to that obtained for the rhenium complex. Absorption effects are much smaller in the former and the metal ion contributes to a smaller percentage of the scattering power, which means the non-metal ions can be located with more accuracy. In addition, data could be collected to a higher $\sin\theta/\lambda$ limit in the technetium case, and a higher percentage of the reflections could be observed. As a result of this increased accuracy more may be said about the structural details in the technetium complex. While the same details are also noted in $TPP[Re(CO)_3]_2$, the significance of these are harder to judge because of the lower accuracy. In the subsequent discussion, the value found in $TPP[Tc(CO)_3]_2$ is used unless other-

wise specified. Bond lengths and angles for both complexes are listed in Tables 8 and 9.

A stereoview of $TPP[Tc(CO)_3]_2$ is shown in Figure 7. For comparison the structure of $TPP[Re(CO)_3]_2$ is shown in Figure 8. Figure 9 shows the coordination sphere and the bond lengths involving the metal atom in both complexes. In each case the metal atoms are situated 1.42 Å from the plane defined by the four pyrrole nitrogen atoms. The metal ions are not positioned directly over the center of the macrocycle, but are set to one side such that each metal ion is bonded to three nitrogen atoms. N(2) is bonded to both metal ions. The distances from the metal ion to the fourth nitrogen atom are 3.230 and 3.208 Å for the rhenium and technetium complexes respectively. The M-N(1) distance is 2.16 Å in both cases. The two M-N(2) bonds are much longer, averaging 2.39 Å in both complexes. The M-C bond lengths appear to be normal. There is a small but significant difference in the M-M distances, with the Tc-Tc distance (3.101(1) Å) being 0.02 Å shorter that the Re-Re distance (3.126(1) Å). This small difference in the covalent radii of congeners in the second and third row transition metal series can be attributed to the lanthanide contraction effect.

The porphyrin macrocycle is highly distorted. The distortion is such that if one considers the mean plane of the macrocycle, pyrrole ring 1, [N(1), C(1)-C(4)], is "bent" towards the metal atom to which it is coordinated while pyrrole ring 2, [N(2), C(6)-C(9)], lies almost in the mean plane of the macrocycle. The individual pyrrole rings are quite planar, but the angle between the least squares planes of the two adjacent rings is 17.0° in both complexes. Another measure of the bending

is the perpendicular distance of an atom in one pyrrole ring from the least squares plane defined by the equivalent ring across the macrocycle. Thus, N(1)' lies 1.83 Å from the plane of pyrrole ring 1. N(2)' lies 0.34 Å from the plane of pyrrole ring 2. (The primes indicate an atom related by a center of symmetry). Table 10 lists various least squares planes of interest and the interplanar angles for the two complexes, $TPP[Tc(CO)_3]_2$ and $TPP[Re(CO)_3]_2$.

The distortion of the macrocycle leads to unusual distances between opposite pyrrole nitrogen atoms. The optimum value for the diameter of the "hole" of an undistorted metalloporphyrin complex has been estimated[53] to be 4.02 Å. The N(1)-N(1)' distance is unusually long (4.506(3) Å in $TPP[Tc(CO)_3]_2$). It is caused by the large deviation of pyrrole ring from the mean plane of the macrocycle. The N(2)-N(2)' distance is unusually short (3.672(4) Å in the ditechnetium complex). This shortening apparently arises so that octahedral coordination may be attained. It is of interest to note that the two Cm-Cm distances are approximately the same and similar to those found in monometallic porphyrin complexes.[53]

Figure 10 shows a schematic drawing of the macrocycle and the averaged bond lengths and angles. Because pyrrole rings 1 and 2 are not chemically equivalent, they must be considered separately in the averages. Also shown in Figure 10 is the nomenclature used for the different type of carbon atoms.

The involvement of N(2) in two coordination bonds might be expected to affect the double bond character of the Cα-N(2) bonds. This effect is indeed seen as the average Cα-N(2) distance is 1.416(3) Å as compared to the Cα-N(1) distance of 1.359(4) Å. The latter distance is typical of

that found in normal metalloporphyrin complexes.[53] In addition, the [C(6)-N(2)-C(9)] angle is 2.9° less than the [C(1)-N(1)-C(4)] angle.

To a lesser extent the bond lengths and angles around Cα atoms on pyrrole ring 2 are affected. The average Cα-Cβ distance is slightly smaller than the analogous bond length in pyrrole ring 1. In this case, however, the significance of these differences may only be classified as marginal. In normal metalloporphyrin complexes, the Cα-Cβ distance has been found to be remarkably constant at approximately 1.44 Å.[53] The Cβ-Cα-Cm and N-Cα-Cm angles are considerably different in the two rings, but this is probably a factor of the distortion of the macrocycle.

As is normal for metallo-tetraphenylporphine complexes,[4] the phenyl rings are rotated considerably out of the plane of the macrocycle. The angles between the planes of the phenyl rings and the plane of the macrocycle are listed in Table 10. The average carbon-carbon bond distance in the two phenyl rings is 1.37(3) and 1.377(9) Å for the rhenium and technetium complexes respectively.

One O-O intermolecular contact is unusually short. This is the contact O(1)-O(3) (x"=x, y"=0.5-y, z"=-0.5 +z) which is 2.91Å. long. This distance is greater than the sum of the van der Waals radii. This contact does not appear to have any effect on the molecular structure. All other contacts are greater than 3.35Å with most being greater than 3.5Å.

DISCUSSION

Although high oxidation state rhenium complexes of porphyrin[33] and phthalocyanine[54] have been prepared, the low oxidation state, out-of-plane, rhenium and technetium complexes of porphyrin are synthesized differently by using the metal carbonyl method.[25] The new metalloporphyrin

complexes are unusual in coordination and stereochemistry. Both the homo- and heterodinuclear metalloporphyrin complexes of Re(I) and Tc(I) are prepared for the first time. In these dimetallic complexes the porphyrin acts as a hexadentate ligand, while in the analogous monometallic complexes, the porphyrin acts as a tridentate ligand. These are rather unusual coordination numbers for the porphyrin ligand.[3] A similar unusual coordination number has also been observed in low oxidation state, out-of-plane rhodium porphyrin complexes.[42] In these rhodium complexes the porphyrin acts either as a bidentate or a tetradentate ligand.

Octahedral[44] coordination was observed in the unusual metalloporphyrin complexes of Re(I) and Tc(I); each metal ion is bonded to three carbonyls and three adjacent pyrrole nitrogen atoms of the porphyrin ring. However, square planar[42] coordination was found in the unusual metalloporphyrin complexes of Rh(I), each metal ion being bonded to two carbonyls and two pyrrole nitrogen atoms. The low oxidation states of these metal ions are presumably stabilized by the carbonyl ligands, and their electronic configurations are consistent (except for the Rh(I) complexes) with the eighteen-electron rule.[55] Among these out-of-plane unusual metalloporphyrin complexes, only the Re(I) complexes are stable compounds; both the Rh(I) and Tc(I) complexes are thermally unstable. A novel thermal disproportionation reaction (Figure 6) of (H-MP)$Tc(CO)_3$ and the thermal instability of $MP[Tc(CO)_3]_2$ have been described earlier. The out-of-plane, dimetallic porphyrin complex of Rh(I) is also unstable with respect to the in-plane, square planar Rh(III) porphyrin complex.[41] The mechanisms of these unusual reactions are unknown. However, dissociation and recombination of the metal-carbonyl moieties with the porphyrin ligand could explain the thermal disproportionation of (H-MP)$Tc(CO)_3$ to $Mp[Tc(CO)_3]_2$ and H_2MPIXDME.

The out-of-plane, monorhenium complex of porphyrin can be used as a model for the proposed "sitting-atop" intermediate in metalloporphyrin formation.[56,57] Although homo- and heterodinuclear, out-of-plane, metalloporphyrin complexes of Re and Tc were prepared through the monorhenium complex by further reaction with $Re_2(CO)_{10}$ and $Tc_2(CO)_{10}$, the incorporation of additional mono- and divalent heavy metal ions (Ag^+, Hg^{++}, and Pb^{++}) to the monorhenium porphyrin complex did not produce stable complexes.[48] It is of interest that an unusual, stable, out-of-plane, metalloporphyrin complex of mercury (II) was prepared simply by the reaction of mercuric acetate with porphyrin in tetrahydrofuran and methylene chloride. This new metalloporphyrin complex was proposed to have an unusual "double-sandwich" structure.[58] Still another mercury porphyrin, this one containing two mercury (II) atoms per porphyrin, has been prepared.[59] It seems to resemble the bimetallic complexes of rhenium(I) and technetium(I). Further comparisons may prove useful.

The intramolecular rearrangement[46] of the metal-carbonyl moiety among the pyrrole nitrogen atoms in the porphyrin ring is the first fluxional behavior reported for the out-of-plane metalloporphyrins such as these. However, both the inter- and intramolecular ligand site exchanging[60] reactions were responsible for the variable-temperature pmr spectral changes in the ruthenium monocarbonyl porphyrin complex coordinated with other nitrogen bases. Rotation of phenyl rings[61,62] in the substituted tetraphenylporphine complexes of Ru(II) and In(III) was also observed by variable-temperature pmr studies. These three different types of fluxional behaviors are very unusual for metalloporphyrins.

One of the major reasons for single crystal X-ray diffraction analyses of $TPP[Re(CO)_3]_2$ and $TPP[Tc(CO)_3]_2$ was to investigate the possible existence of a metal-metal bonding through the porphyrin "hole" to form a

"skewered compound". However, it would appear that for the following reasons the metal-metal interactions, if present, are weak. Firstly, the M-M distance (~3.1Å) is rather large for a metal-metal bond. Most Re-Re single bond distances are approximately 2.7 Å long,[63] although a value of 3.02 Å has been reported for $Re_2(CO)_{10}$.[64] Secondly, the macrocycle is highly distorted in a way which would maximize the M-M distance. Thirdly, the eighteen-electron rule[55] is fulfilled without postulating a metal-metal bond.

EXPERIMENTAL SECTION

Materials

Hemin was purchased from Sigma Chemical Co.; dirhenium decacarbonyl, $Re_2(CO)_{10}$, and ditechnetium decacarbonyl, $Tc_2(CO)_{10}$, were purchased from Pressure Chemical Co.; $Tc_2(CO)_{10}$ is a radioactive material with radioactivity of 5 μc/mg ($_{43}Tc^{99}$: β^-, 0.292 MeV; half-life, 2.12×10^5 years). Talcum powder was purchased from Fisher Scientific Co., and Sephadex LH-20 was obtained from Pharmacia Fine Chemicals. Decahydronaphthalene (decalin) was purchased from J. T. Baker Chemical Co., treated with concentrated sulfuric acid, neutralized with sodium bicarbonate solution, washed with distilled water, dried over anhydrous calcium chloride overnight, filtered, and further dried over sodium wire; finally it was distilled under vacuum and stored in a Schlenk tube under argon before use. 1,1,2,2-Tetrachloroethane was purchased from Eastman Kodak Co., dried over phosphorus pentoxide, and distilled under vacuum before use. Other organic solvents were commercial reagent grade and were used without further purification.

Physical Measurements.

Elemental analyses and molecular weight determinations were performed by Schwarzkopf Microanalytical Laboratory, Woodside, N. Y. 11377. Visible spectra were measured with a Cary 14 spectrophotometer. Infrared Spectra were measured with a Beckman IR-8 spectrophotometer. Mass spectra were obtained on a CEC 21-104 mass spectrometer. Proton magnetic resonance spectra were obtained using Varian T-60 and HA-100 spectrometers; the latter was equipped with a variable-temperature probe and operated at power levels well below saturation. Temperatures were measured with a thermocouple mounted in the probe which was calibrated with ethylene glycol after each set of spectra.

Preparations.

Mesoporphyrin IX dimethyl ester,[65] H_2MPIXDME, and meso-tetraphenylporphine,[66,67] H_2TPP, were prepared by literature procedures. (Monohydrogen mesoporphyrin IX dimethyl esterato)tricarbonylrhenium(I), (H-MP)-$Re(CO)_3$, (I), μ-[mesoporphyrin IX dimethyl esterato]bis[tricarbonylrhenium(I)], MP$[Re(CO)_3]_2$, (III), μ-[meso-tetraphenylporphinato]bis[tricarbonylrhenium(I)], TPP$[Re(CO)_3]_2$, (IV), and [tricarbonylrhenium(I)]--μ-[mesoporphyrin IX dimethyl esterato]-[tricarbonyltechnetium(I)], $(CO)_3$ReMPTc$(CO)_3$, (V), were prepared as previously reported.[43-45]

[Monohydrogen mesoporphyrin IX dimethyl esterato]tricarbonyltechnetium(I), (H-MP)Tc$(CO)_3$, (VI). A 45.5 mg sample of H_2MPIXDME (7.58×10^{-2} mmol) and 21.25 mg (4.46×10^{-2} mmol) of $Tc_2(CO)_{10}$ were mixed in 10 ml of decalin and heated under argon in a 150° oil-bath for approximately two hours. Completion of the reaction was determined by visible spectroscopy. When absorption at 388 nm (Soret band) and 473 nm reached maxima, the

reaction was stopped. The decalin solution was cooled, centrifuged, and decanted, and the supernatant evaporated to dryness under vacuum by using a Molecular Still apparatus. The resulting solid was then dissolved in benzene and chromatographed on a talcum column. Three bands were eluted from the column by benzene/cyclohexane (50/50), dichloromethane, and acetone respectively. A small amount of chocolate colored material was followed by a large pale green band; and finally by a small amount of red compound. Visible spectroscopy showed the first and third bands to be $MP[Tc(CO)_3]_2$, (VII), and H_2MPIXDME. A dichloromethane solution of the second band was evaporated to small volume under a stream of nitrogen, centrifuged, and decanted. The supernatant was evaporated to dryness and washed with n-pentane to give an air stable, dark greenish brown solid of VI (24.15 mg, 41.0% yield), mp 181-182°. Anal. Calcd. for $TcC_{39}H_{41}N_4O_7$: N, 7.22; Tc, 12.75; Mol. Wt., 776.8. Found: N, 7.34; Tc, 12.37; Mol. Wts., 767 (measured by vapor pressure osmometry in chloroform).

μ-[Mesoporphyrin IX dimethyl esterato]bis[tricarbonyltechnetium(I)], $MP[Tc(CO)_3]_2$, (VII). The preparation of this compound was similar to that of VI, except the ratio of reactants was changed. H_2MPIXDME (20.6 mg, 3.49×10^{-2} mmol) and $Tc_2(CO)_{10}$ (19.5 mg, 4.08×10^{-2} mmol) were mixed in 10 ml of decalin and heated under argon in a 150° oil-bath for approximately five hours. Completion of the reaction was determined by visible spectroscopy; stepwise absorption changes of the reaction mixture were observed as shown in Figure 3. When the absorptions at 396 nm (Soret band) and 507 nm reached maxima, the reaction was stopped. The decalin solution was centrifuged, decanted, and evaporated in vacuo; the resulting solid was dissolved in benzene and chromatographed on a talcum column. A large chocolate colored band was eluted with a benzene/cyclohexane (50/50) solution. This

solution was evaporated to dryness, dissolved in dichloromethane, centrifuged, and decanted. Finally it was evaporated to dryness and washed with n-pentane to give a dark reddish brown solid of VII (21.20 mg, 65.8% yield), mp 227-229°. Anal. Calcd. for $Tc_2C_{42}H_{40}N_4O_{10}$: C, 52.60; H, 4.18; N, 5.84; Tc, 20.65; Mol. Wt., 958.0. Found: C, 52.44; H, 4.08; N, 5.92; Tc, 20.54; Mol. Wt., ~1062 (measured by vapor pressure osmometry in acetone).

μ-[meso-tetraphenylporphinato]bis[tricarbonyltechnetium(I)], TPP[Tc(CO)$_3$]$_2$, (VIII). The preparation of this compound was similar to that of VII, except the porphyrin ligand was changed. H_2TPP (23.0 mg, 3.75×10^{-2} mmol) and $Tc_2(CO)_{10}$ (20.6 mg, 4.31×10^{-2} mmol) were mixed in 10 ml of decalin and refluxed under argon for approximately two hours. Completion of the reaction was determined by visible spectroscopy. The visible spectrum of this mixture after two hours refluxing was rather similar to that of VII. The crude product was isolated from the decalin solution in a similar manner as that of VII, and chromatographed on a Sephadex LH-20 column. A reddish brown colored band was eluted with a benzene/cyclohexane (50/50) solution. This solution was concentrated to small volume, centrifuged, and decanted. Finally it was evaporated to dryness, washed with n-pentane, and crystallized from dichloromethane/chloroform solution to give reddish brown crystals of VIII (23.81 mg, 65.1% yield), mp 323-325°. These crystals were used for X-ray diffraction analyses.

[Monohydrogen meso-tetraphenylporphinato]tricarbonylrhenium(I), (H-TPP)-Re(CO)$_3$, (II). A 207.5 mg sample of H_2TPP (0.338 mmol) and 100 mg (0.157 mmol) $Re_2(CO)_{10}$ in 20 ml of decalin were refluxed under argon for approximately three hours. Completion of the reaction was determined by visible spectroscopy. The crude product was isolated from the decalin solution in a similar manner as that of VII, and chromatographed on a Sephadex LH-20 column. A yellowish brown colored band was eluted with cyclohexane. This solution was concentrated

to small volume, centrifuged, and decanted. The supernatant was evaporated to dryness, washed with n-pentane, and crystallized from absolute alcohol/chloroform solution to give an air stable, dark greenish brown solid of II (140.3 mg, 50.6% yield), mp 302-304°. Anal. Calcd. for $ReC_{47}H_{29}N_4O_3$: C, 63.80; H, 3.29; N, 6.34; Re, 21.08; Mol. Wt., 883.2. Found: C, 63.78; H, 3.57; N, 6.47; Re, 21.43; Mol. Wt., 840 (in dibromomethane).

X-ray Study

Crystals of μ-[meso-tetraphenylporphinato]bis[tricarbonylrhenium(I)] $TPP[Re(CO)_3]_2$, IV, $C_{50}H_{28}O_6N_4Re_2$, were grown from a dioxane solution. The crystals grew as elongated plates with the most prominent faces being {100}, and bounded by {010} and {011}. The crystal used for intensity measurements had dimensions 0.03 and 0.08 mm in the direction of a and b respectively, while the long dimension (approximately parallel to c) was 0.28 mm. The crystals appear green in reflected light.

Crystals of μ-[meso-tetraphenylporphinato]bis[tricarbonyltechnetium(I)] $TPP[Tc(CO)_3]_2$, VIII, $C_{50}H_{28}O_6N_4Tc_2$, exhibited two different crystal habits. One form was the same as that found for the rhenium compound while the other form was much more complex. These crystals were again plates with the prominent faces being of the form {100}, and bounded by {011} and the faces [111], [$\bar{1}1\bar{1}$], [1$\bar{1}$1], and [$\bar{1}\bar{1}\bar{1}$]. Two corners were truncated by faces of the form {010}. Crystals of this form were grown from chloroform and dichloromethane. The crystal chosen for intensity measurements was of this form and had dimensions of 0.18 x 0.37 x 0.32 mm. Both forms appeared green in reflected light and gave identical space group and cell dimensions. Crystals of both complexes were mounted in glass capillaries.

Crystal data for both the rhenium and technetium complexes are listed in Table 4. Also listed are some of the experimental conditions used in the intensity measurements. Cell dimensions were determined by least squares, minimizing the differences between observed and calculated 2θ values. For both complexes MoKα radiation, monochromatized by pyrolytic graphite, was used. The 2θ values were measured on a Syntex-Datex automated four-circle diffractometer. In the case of $TPP[Tc(CO)_3]_2$, the 2θ values for 19 $MoK\alpha_1$

(λ=0.70926 Å) were measured. For six of these, the $K\alpha_1$-$K\alpha_2$ doublet was sufficiently resolved to measure the 2θ values for the $K\alpha_2$ reflections (λ=0.71354 Å). In the case of $TPP[Re(CO)_3]_2$, the doublet was not well resolved and 40 2θ values were measured assuming the wavelength to be Mo $K\bar{\alpha}$ (λ=0.71069 Å). The densities were determined by the flotation method in an aqueous thallous formate solution. The two complexes are isomorphous. In both cases the choice of space group, $P2_1/c$, was uniquely determined by the systematic absences.

Intensity data were collected on the Datex-Syntex diffractometer. The data in each case were collected by the θ-2θ scan method, monitoring the intensity scale by remeasuring a group of five standard reflections periodically. For both complexes there were no significant or systematic trends in the intensities of these check reflections and no corrections were made. Backgrounds at either end of the scan range were collected for half the scan time. Only reflections with $I \geq 3\sigma_I$ were used in the analyses. The standard deviation σ_I was determined in terms of the statistical variances of the counts as $\sigma_I^2 = \sigma_I^2$ (count) + $K^2(S + B1 + B2)^2$, where S, B1, and B2 are the observed counts for the scan and two backgrounds respectively. σ_I^2 (count) is the variance determined purely from counting statistics. The values of K, the so-called stability constant, were determined empirically. The intensities were corrected for coincidence using the method of Sletten, Sletten and Jensen.[68] Absorption effect corrections were applied to both complexes. In the case of $TPP[Tc(CO)_3]_2$, where the corrections were small, a numerical integration method was used. In the case of the rhenium complex, the more accurate analytical correction technique of DeMeulenaer and Tompa was used.[69]

Transmission factors ranged from 0.61 to 0.86 for $TPP[Re(CO)_3]_2$ and from 0.85 to 0.93 for $TPP[Tc(CO)_3]_2$. Structure factors were calculated in the usual way, assuming an ideally imperfect monochromator.

Determination and Refinement of the Structures

Because there are only two molecules in the unit cell of space group $P2_1/c$, the complex in both cases must be centrosymmetric. However, no atom is constrained to be at a special position. The position of the metal atoms were found in each case from a Patterson synthesis. The positions of the remaining 30 non-hydrogen atoms in the asymmetric unit were found from a series of ΔF Fourier maps.

Least squares refinement using block diagonal and finally full matrix methods[70] was carried out. The function minimized was $\Sigma w(Fo-Fc)^2$, where $w=1/\sigma_F^2$ Initially isotropic temperature factors were used, but in later refinement cycles all non-hydrogen atoms were assumed to have anisotropic thermal motion.

After several cycles of refinement of the non-hydrogen atoms, ΔF syntheses were calculated in an effort to locate hydrogen atoms. In the case of the rhenium complex, the positions of most of the 14 hydrogen atoms could not be located with certainty, so calculated positions for all of them were used and were not refined by least squares. A bond length of 1.0 Å was assumed. In the case of the technetium complex, the hydrogen atoms could be located and these positions were refined, assuming isotropic thermal motion.

In the final cycles of full matrix least squares refinement, computer memory limitations necessitated refining the parameters in two blocks. In

the first block, all atoms except those belonging to the phenyl groups were refined. In the other block, the metal atom and the atoms of the phenyl group were refined. The final R values are given in Table 4.

Corrections were made for anomalous dispersion for the metal atom in each case.[71] Scattering factors were from the International Tables.[72] The metal ions were assumed to be in the zero ionization state.

The data were examined by the method of Housty and Clastre.[73] No evidence of secondary extinction was found and no correction for this effect was made.

Final difference syntheses were calculated for both compounds. In the case of TPP[$Tc(CO)_3$]$_2$ the maximum residual elution density was 0.5 e/A^3, while for TPP[$Re(CO)_3$]$_2$ the maximum peak was 1.5 e/A^3. Both peaks were near the metal ions and were not considered of any physical significance.

The computer programs used have been previously listed.[74,75] The final positional and thermal parameters are listed in Tables 5 and 6, while the root-mean-square components of thermal displacement along the principal axis of the thermal ellipsoids are given in Table 7. Tables of observed and calculated structure factors are available.[76]

Acknowledgement. This research project was supported in part by both the National Science Foundation under Grant no. GP-28685 and the Office of Naval Research under Grant no. NR 356-559. The authors wish to thank Dr. Allen E. Gebala for many helpful discussions. Crystallographic investigations were supported by the Robert A. Welch Foundation Grant A-328 and the Texas Agricultural Experiment Station. Crystallographic

calculations were facilitated by the CRYSNET system, supported by the National Science Foundation GJ33248X.

Supplementary Material Available. A listing of structure factor amplitudes will appear following these pages in the microfilm edition of this volume of the journal. Photocopies of the supplementary material from this paper only or microfiche (105 x 148 mm, 24x reduction, negatives) containing all of the supplementary material for the papers in this issue may be obtained from the Journals Department, American Chemical Society, 1155 16th St., N. W., Washington D. C. 20036. Remit check or money order for $3.00 for photocopy or $2.00 for microfiche, referring to code number JACS-75-0000.

REFERENCES

1. Unusual Metalloporphyrins XXIII.

2. Present Address: Chemistry Department, Seton Hall University South Orange, New Jersey 07079

3. J. E. Falk, "Porphyrins and Metalloporphyrins", Elsevier, N.Y., 1964.

4. E. B. Fleischer, Accounts Chem. Res., 3, 105 (1970).

5. P. Hambright, Coord. Chem. Rev., 6, 247 (1971).

6. L. J. Boucher, ibid., 7, 289 (1972).

7. D. Ostfeld and M. Tsutsui, Accounts Chem. Res., 7, 52 (1974).

8. A. D. Adler, ed., "The Chemical and Physical Behavior of Porphyrin Compounds and Related Structures", Ann. New York Acad. Sci., Vol. 206, 1973.

9. C. K. Chang and T. G. Traylor, J. Amer. Chem. Soc., 95, 5810, 8475 8477 (1973).

10. D. V. Stynes, H. C. Stynes, B. R. James and J. A. Ibers, ibid., 95, 4087 (1973).

11. B. B. Wayland, J. V. Minkiewicz and M. E. Abd-Elmageed, ibid., 96, 2795 (1974).

12. J. P. Collman, R. R. Gagne and C. A. Reed, ibid., 96, 2629 (1974).

13. L. P. Vernon and G. R. Seely, eds., "The Chlorophylls: Physical, Chemical, and Biological Properties", Academic Press, New York and London, 1966.

14. E. Antonini and M. Brunori, "Hemoglobin and Myoglobin in their Reactions with Ligands", North-Holland/American Elsevier, 1971.

15. R. Lemberg and K. Barrett, "Cytochromes", Academic Press, London and New York, 1973.

16. E. L. Smith, "Vitamin B_{12}", 3rd ed., John Wiley & Sons, Inc., New York, 1965.

17. G. N. Schrauzer, Accounts Chem. Res., 1, 97 (1968).

18. A. Goldberg and C. Rimington, "Diseases of Porphyrin Metabolism", Thomas, Springfield, 1962.

19. F. Gutmann and L. E. Lyons, "Organic Semiconductors", Wiley, N. Y. 1967.

20. A. D. Adler, J. Polymer Sci., Part C, 29, 73 (1970).

21. J. P. Macquet and T. Theophanides, Can. J. Chem., 51, 219 (1972).

22. G. A. Kyriazis, H. Balin, and R. L. Lipson, Amer. J. Obstet. Gynecol., 376 (1973).

23. E. B. Fleischer and M. Krishnamurthy, J. Amer. Chem. Soc., 94, 1382 (1972).

24. C. P. Wong, R. F. Venteicher, and W. D. Horrocks, Jr., ibid., 96, 7149 (1974).

25. M. Tsutsui, M. Ichikawa, F. Vohwinkel, and K. Suzuki, ibid., 88, 854 (1966).

26. M. Tsutsui, R. A. Velapoldi, K. Suzuki, F. Vohwinkel, M. Ichikawa, and T. Koyano, ibid., 91, 6262 (1969).

27. E. B. Fleischer and N. Sadasivan, Chem. Comm., 159 (1967).

28. B. C. Chow and I. A. Cohen, Bioinorg. Chem., 1, 57 (1971).

29. N. Sadasivan and E. B. Fleischer, J. Inorg. Nucl. Chem., 30, 591 (1968).

30. J. W. Buchler, G. Eikelmann, L. Puppe, K. Rohbock, H. H. Schnechage, and D. Weck, Liebigs Ann. Chem., 745, 135 (1971).

31. A. D. Adler, F. R. Longo, F. Kampas, and J. Kim, J. Inorg. Nucl. Chem., 32, 2443 (1970).

32. J. W. Buchler and K. Rohbock, Inorg. Nucl. Chem. Lett., 8, 1073 (1972).

33. J. W. Buchler, L. Puppe, K. Rohbock, and H. H. Schneehage, Chem. Ber., 106, 2710 (1973).

34. J. W. Buchler and K. Rohbock, J. Organometal. Chem., 65, 223 (1974).

35. J. W. Buchler, L. Puppe, K. Rohbock, and H. H. Schneehage, Ann. New York Acad. Sci., 206, 116 (1973).

36. E. B. Fleischer and T. S. Srivastava, Inorg. Chim. Acta, 5, 151 (1971).

37. T. S. Srivastava and E. B. Fleischer, J. Amer. Chem. Soc., 92, 5518 (1970).

38. J. J. Bonnet, S. S. Eaton, G. R. Eaton, R. H. Holm, and J. A. Ibers, ibid., 95, 2141 (1973).

39. E. B. Fleischer and D. Lavalle, ibid., 89, 7132 (1967).

40. H. Ogoshi, T. Omura and Z. Yoshida, ibid., 95, 1666 (1973).

41. Z. Yoshida, H. Ogoshi, T. Omura, E. Watanabe, and T. Kurosaki, Tetrahedron Lett., 11, 1077 (1972).

42. A. Takenaka, Y. Sasada, T. Omura, H. Ogoshi, and Z. Yoshida, J. Chem. Soc., Chem. Comm., 792 (1973).

43. D. Ostfeld, M. Tsutsui, C. P. Hrung, and D. C. Conway, J. Amer. Chem. Soc., 93, 2548 (1971).

44. D. Cullen, E. Meyer, T. S. Srivastava, and M. Tsutsui, ibid., 94 7603 (1972).

45. M. Tsutsui and C. P. Hrung, ibid., 95, 5777 (1973).

46. M. Tsutsui and C. P. Hrung, ibid., 96, 2638 (1974).

47. L. M. Jackson and S. Sternhell, "Applications of Nuclear Magnetic Resonance Spectroscopy in Organic Chemistry", 2nd Ed., Pergamon, New York, p. 129, 1969.

48. D. Ostfeld, M. Tsutsui, C. P. Hrung, and D. C. Conway, J. Coord. Chem., 2, 101 (1972).

49. F. A. Cotton, Accounts Chem. Res., 1, 257 (1968).

50. M. Tsutsui, D. Ostfeld, and L. Hoffman, J. Amer. Chem. Soc., 93, 1820 (1971).

51. V. W. Day, B. R. Stults, E. L. Tasset, R. O. Day, and R. S. Marianelli, ibid., 96, 2650 (1974).

52. P. A. Loach and M. Calvin, Biochemistry, 2, 363 (1963).

53. J. L. Hoard, Science, 174, 1295 (1971).

54. H. P. Boniecka, Rocz. Chem., 41, 1703 (1967).

55. P. R. Mitchell and R. V. Parish, J. Chem. Educ., 46, 811 (1969).

56. E. B. Fleischer, E. I. Choi, P. Hambright, and A. Stone, Inorg. Chem., 3, 1284 (1964).

57. H. Baker, P. Hambright, and L. Wagner, J. Amer. Chem. Soc., 95, 5942 (1973).

58. M. F. Hudson and K. M. Smith, J. Chem. Soc., Chem. Comm., 515 (1973).

59. M. F. Hudson and K. M. Smith, Tetrahedron Lett., 2223 (1974).

60. S. S. Eaton, G. R. Eaton, and R. H. Holm, J. Organomet. Chem., 39, 179 (1972).

61. W. Bhatti, M. Bhatti, S. S. Eaton, and G. R. Eaton, J. Pharm. Sci., 62, 1574 (1973).

62. S. S. Eaton and G. R. Eaton, J. Chem. Soc., Chem. Commun., 576 (1974).

63. F. A. Cotton, Accounts Chem. Res., 2, 240 (1969).

64. N. I. G. Gapotchenko, N. V. Alekseev, N. E. Kolobova, K. N. Anisimov, I. A. Ronova, and A. A. Johansson, J. Organometal. Chem., 35, 319 (1972).

65. A. H. Corwin and J. G. Erdman, J. Amer. Chem. Soc., 68, 2473 (1946).

66. A. D. Adler, F. R. Longo, J. D. Finarelli, J. Goldmacher, J. Assour, and L. Korsakoff, J. Org. Chem., 32, 476 (1967).

67. G. H. Barnett, M. F. Hudson, and K. M. Smith, Tetrahedron Lett., 2887 (1973)

68. E. Sletten, J. Sletten, and L. H. Jensen, Acta Crystallogr., Sect. B, 25, 1330 (1969).

69. J. De Meulenaer and H. Tompa, Acta Crystallogr., 19, 1014 (1965).

70. W. R. Busing, K. O. Martin, and H. Levy, ORFLS, A Fortran Crystallographic Least-Squares Program, Report ORNL-TM-305, Oak Ridge National Laboratory, Oak Ridge Tenn.

71. D. T. Cromer and D. Liberman, J. Chem. Phys., 53, 1891 (1970).

72. D. T. Cromer, "International Tables for X-ray Crystallography", Vol. IV, In Press.

73. J. Housty and J. Clastre, Acta Crystallogr., 10, 695 (1957).

74. D. L. Cullen and E. F. Meyer, Jr., J. Amer. Chem. Soc., 96, 2095 (1974).

75. D. L. Cullen and E. F. Meyer, Jr., Acta Crystallogr., Sect. B, 29, 2507 (1973).

76. See paragraph at end of paper regarding supplementary material.

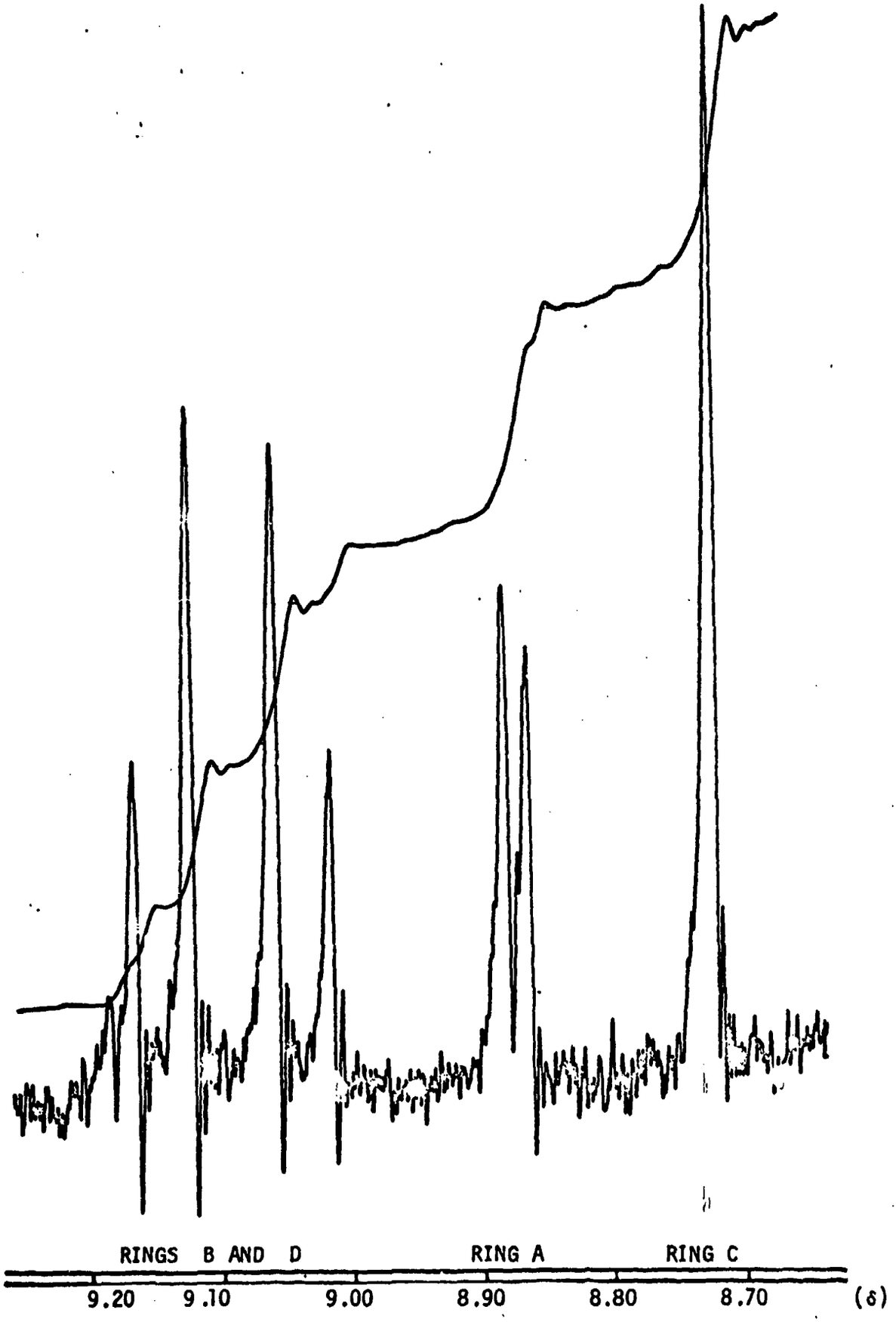

Figure 1. HA-100 nmr spectrum for the pyrrole protons in compound II.

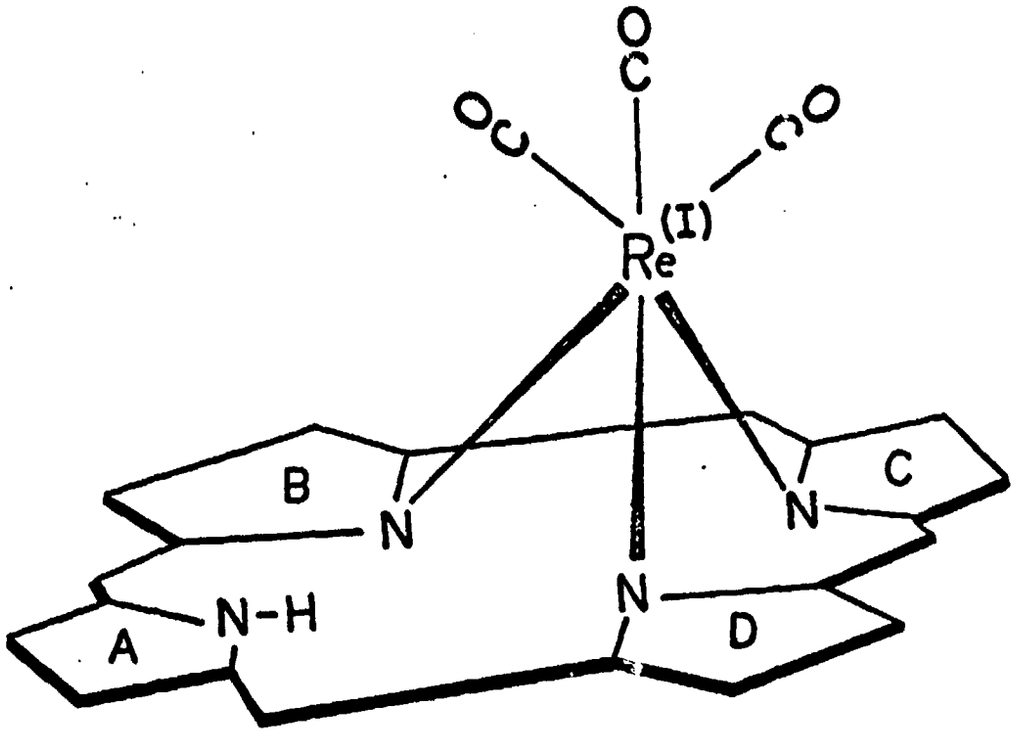

(a)

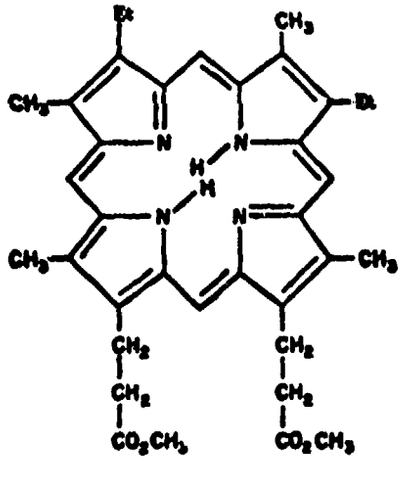

(b)

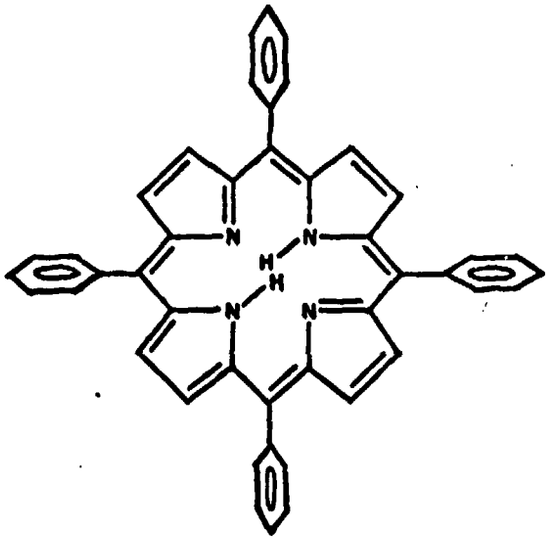

(c)

Figure 2. (a) Proposed structure for $HTPPRe(CO)_3$ and $HMPRe(CO)_3$ (phenyl and alkyl substituents are left out of the porphine ring for clarity); (b) mesoporphyrin IX dimethyl ester, H_2MP; (c) meso-tetraphenylporphine, H_2TPP.

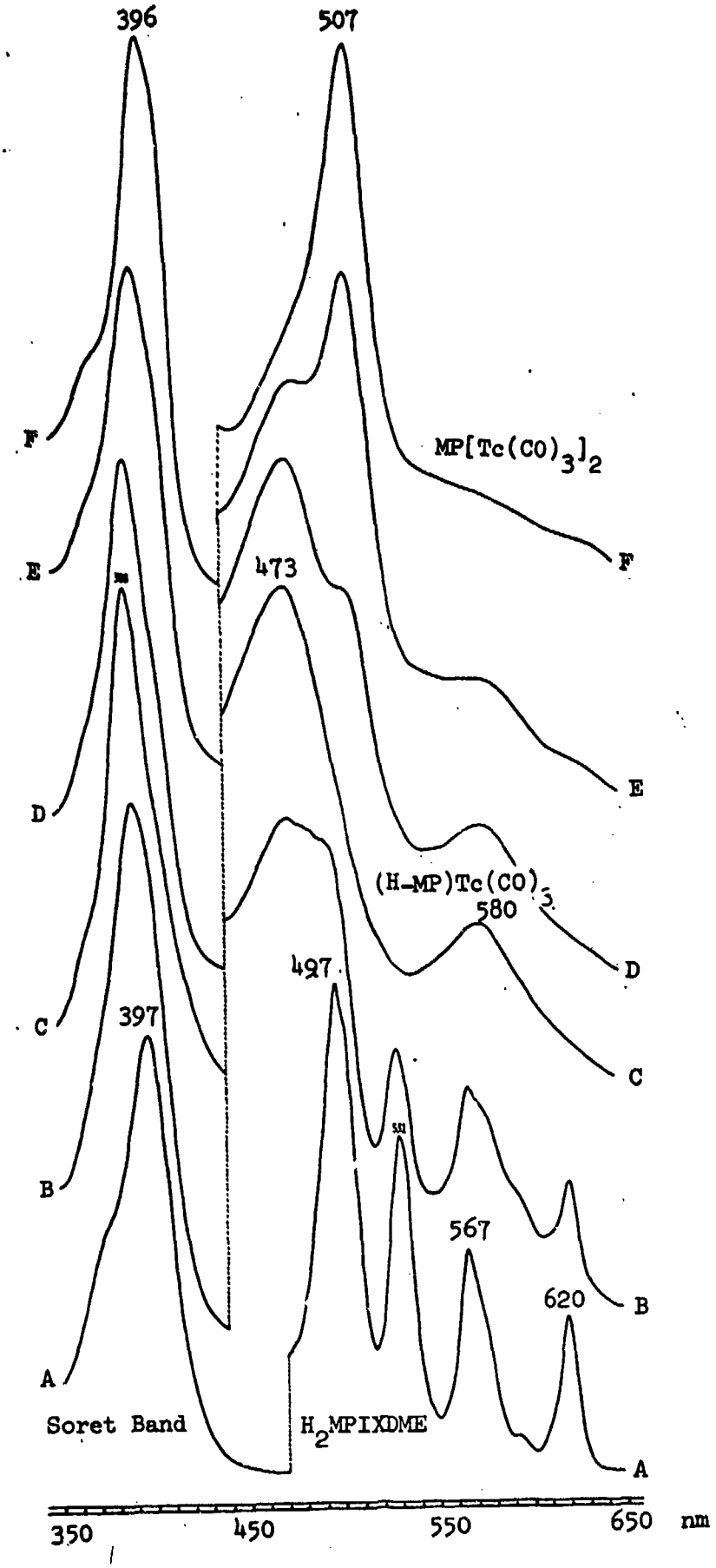

Figure 3. Repeated scan spectrophotometry shows progress of the formation of (H-MP)Tc-$(CO)_3$ and $MP[Tc(CO)_3]_2$.

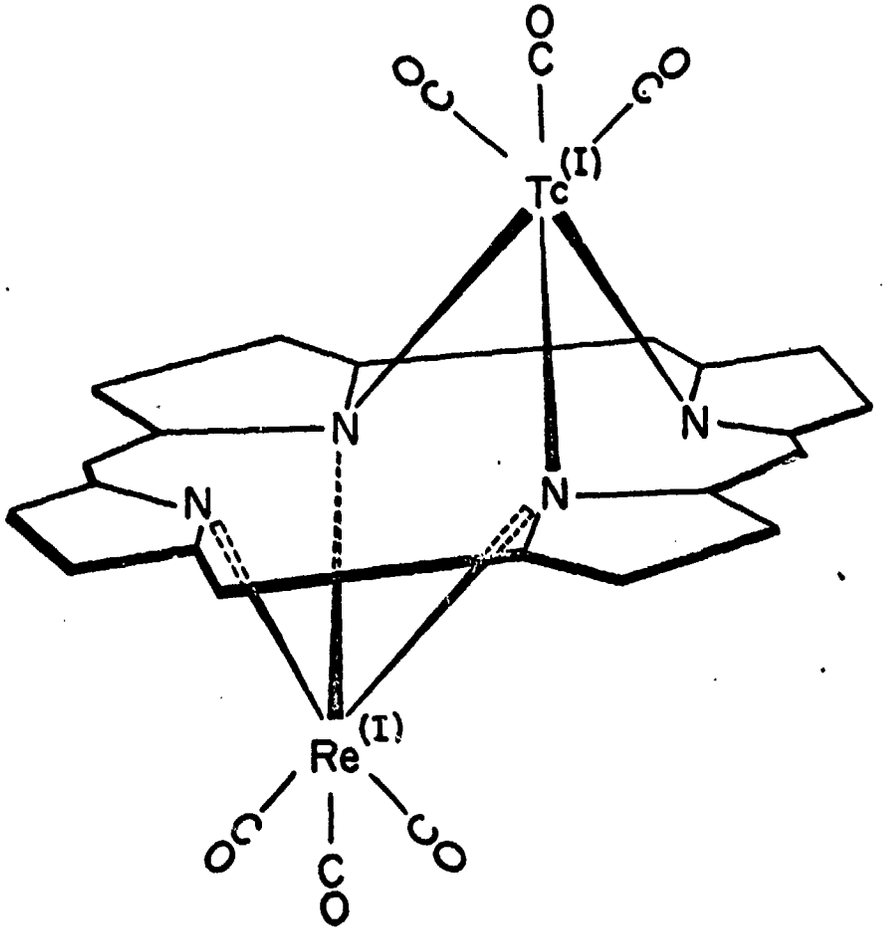

Figure 4. Schematic diagram of $(OC)_3ReMpTc(CO)_3$, V; The alkyl substituents on the porphine ring were omitted for clarity.

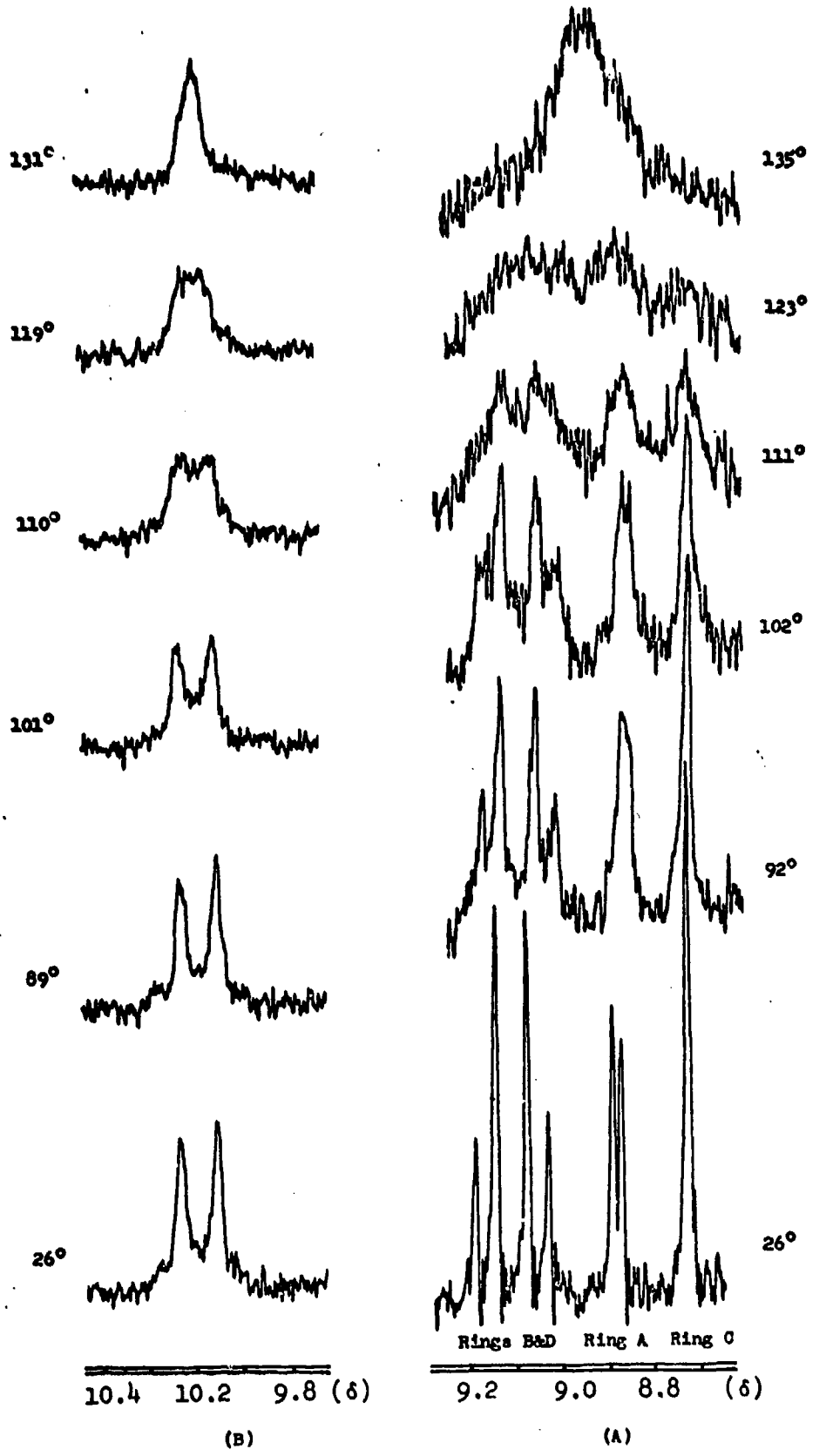

Figure 5. The 100-MHz variable temperature ^1H nmr spectra for (A) β-pyrrole protons of $HTPPRe(CO)_3$ and (B) bridge methine protons of $HMPTc(CO)_3$ (both in $C_2H_2Cl_4$ and temperature in °C).

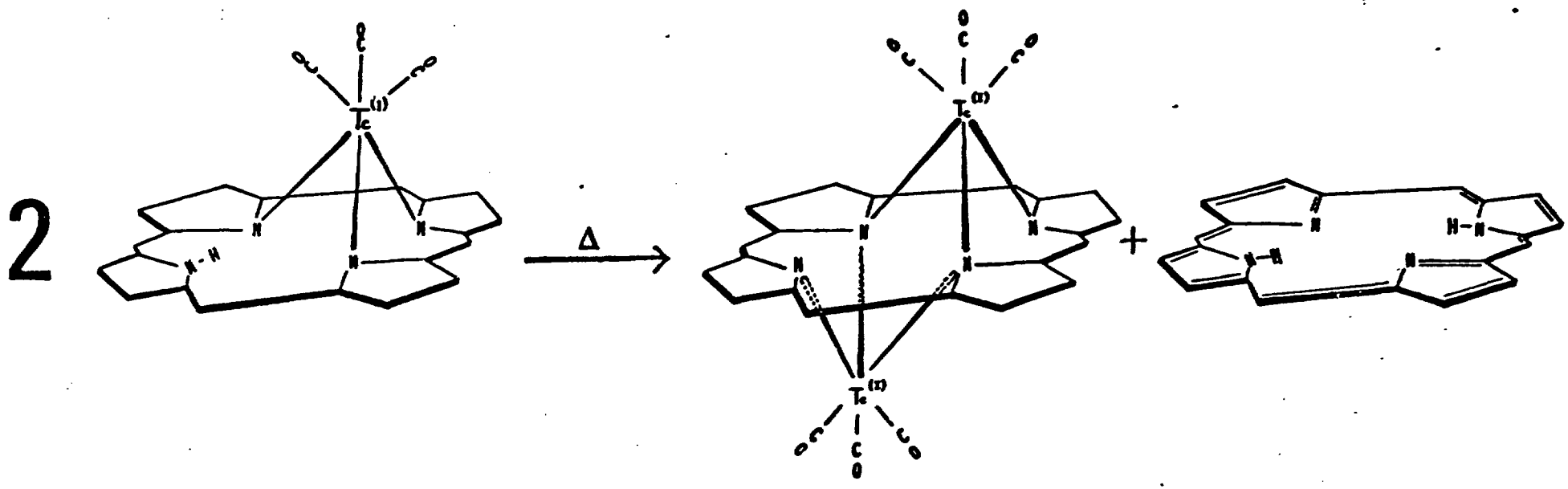

Figure 6. Disproportionating of (H-MP)Tc(CO)$_3$ by heating.

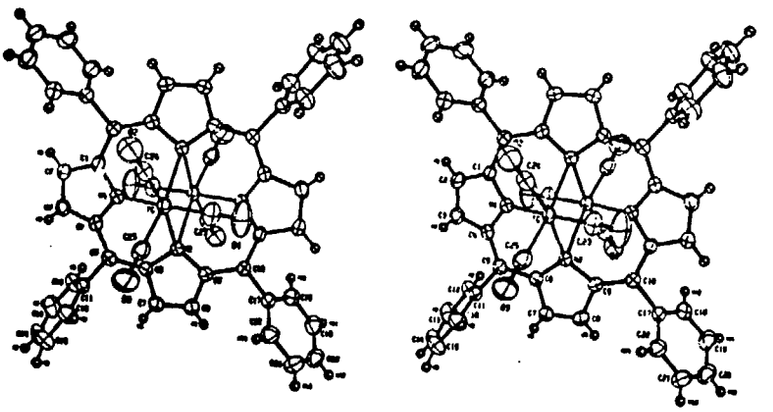

Figure 7. A stereoview of the structure of μ-[meso-tetraphenylporphinato]bis[tricarbonyltechnetium(I)]. Atoms not labeled are centrosymmetrically related. The thermal ellipsoids are drawn for 50% probability, except those of the hydrogen atoms which are not drawn to scale.

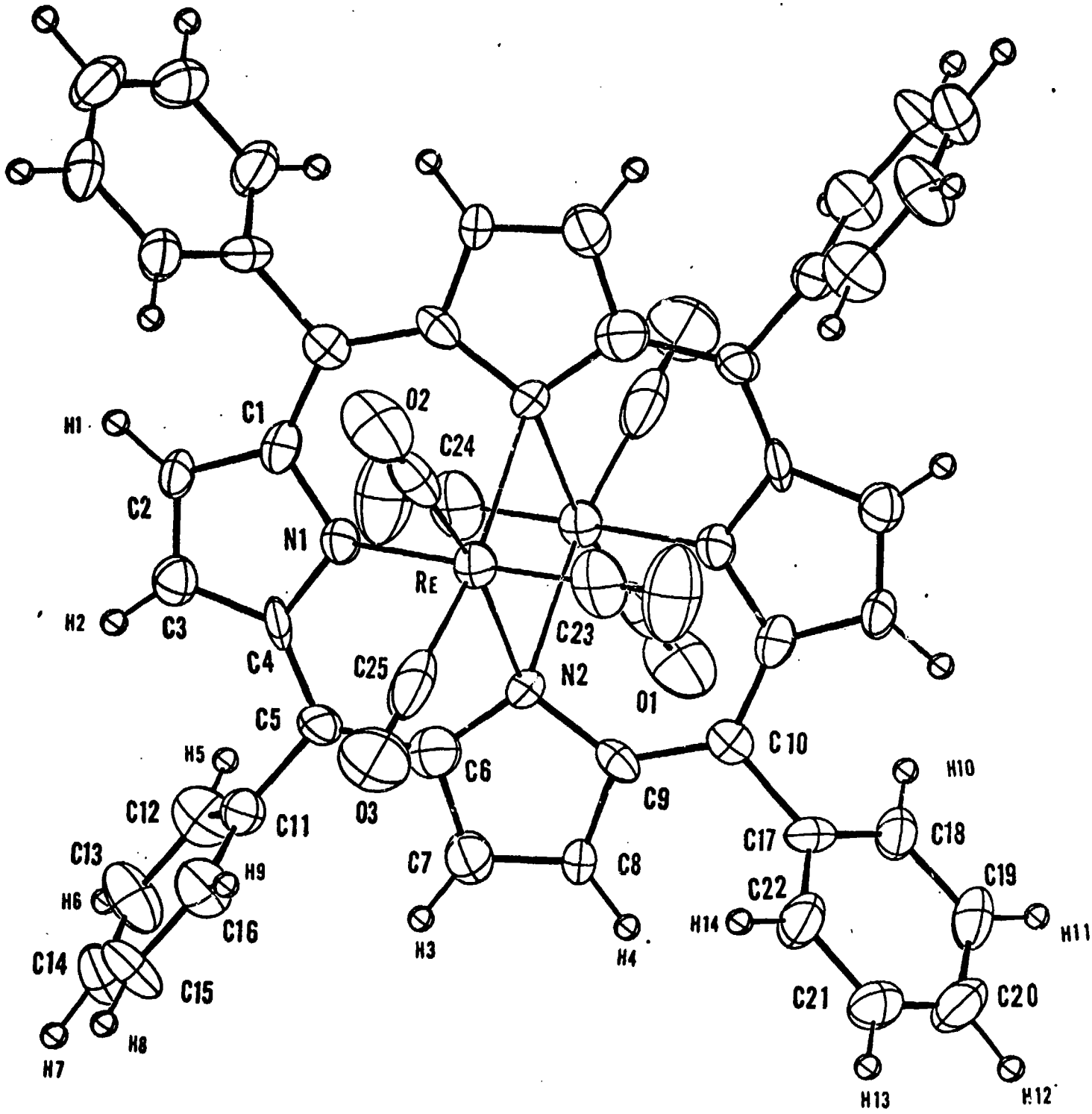

Figure 8. The structure of μ-[meso-tetraphenylporphinato]bis-[tricarbonylrhenium(I)]. The number scheme used is shown. Atoms not labeled are centrosymmetrically related. The thermal ellipsoids are drawn for 50% probability, except for those of the hydrogen atoms which are not drawn to scale.

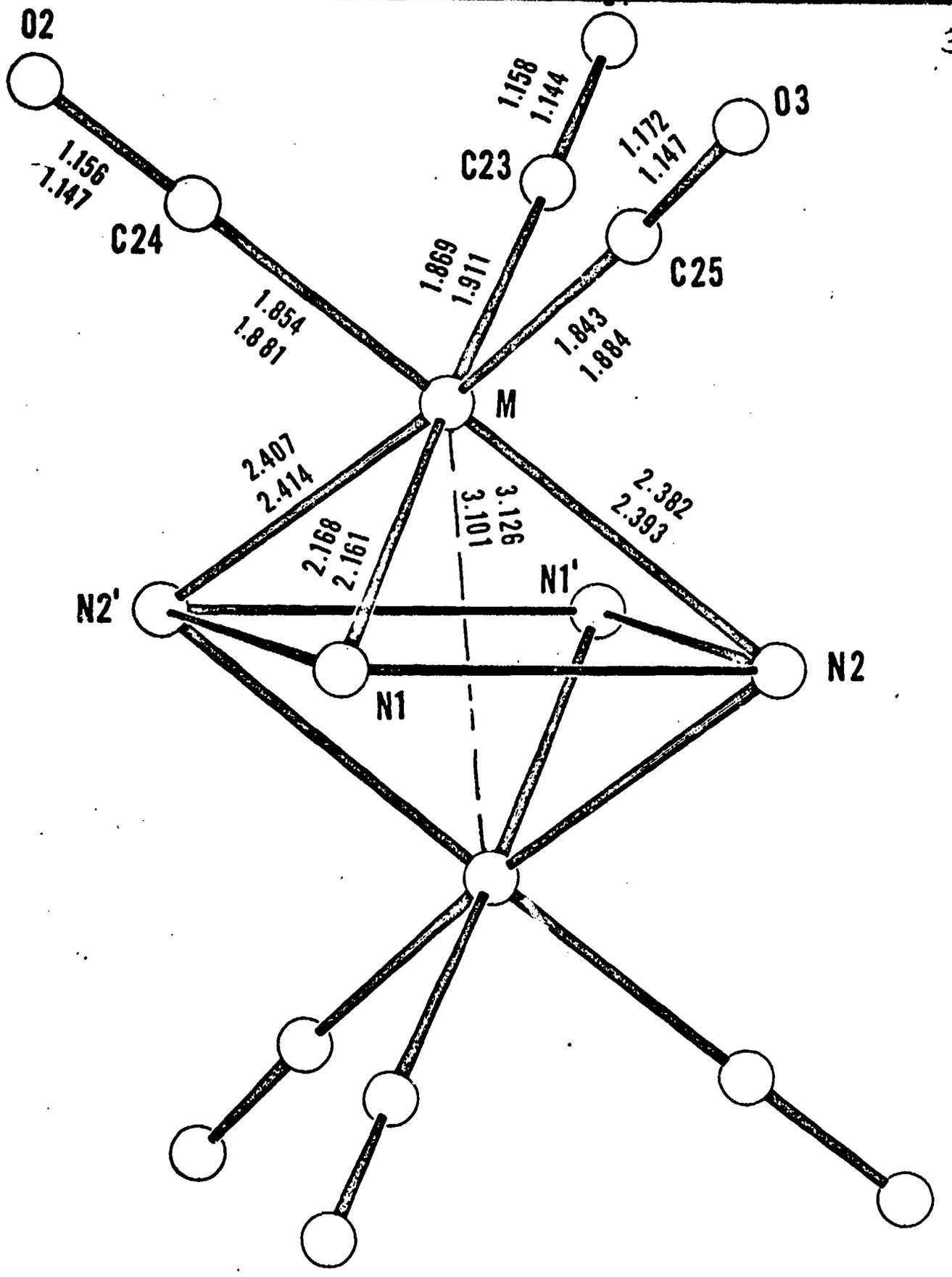

Figure 9. Coordination sphere showing bond distances around the metal atoms in $TPP[Re(CO)_3]_2$ (top value) and $TPP[Tc(CO)_3]_2$ (lower value). The lines between nitrogens signify the plane of the macrocycle. Primed atoms or atoms not labelled are centrosymmetrically related to unprimed atoms.

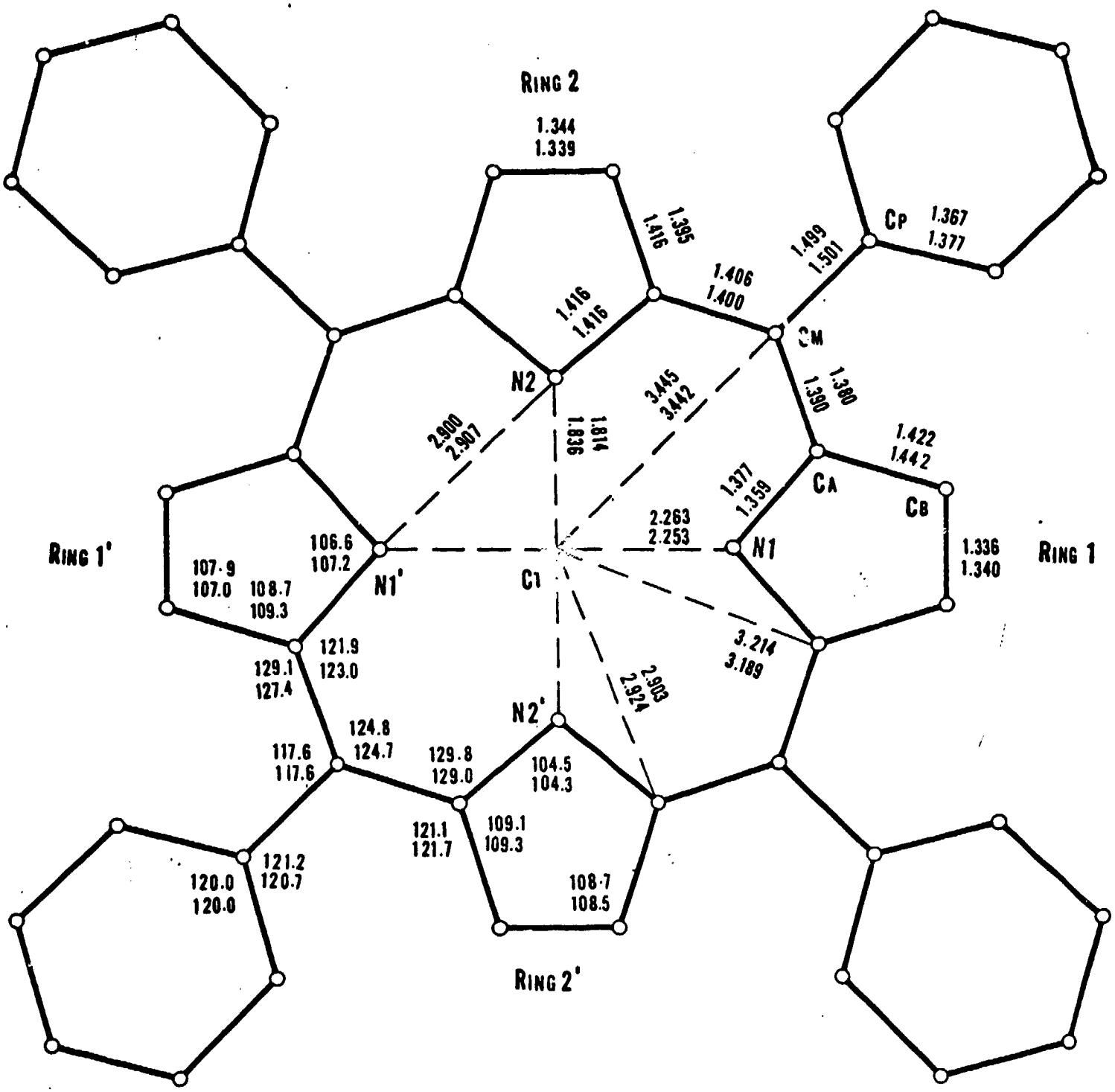

Figure 10. Schematic drawing of the macrocycle showing averaged bond lengths in angstroms and angles in degrees as found in $TPP[Re(CO)_3]_2$ (top value) and $TPP[Tc(CO)_3]_2$ (lower value). Also shown is the notation for different types of carbon atoms.

Table 1. Spectral data for unusual metalloporphyrin complexes, I-IX.

No.	Compound	M.P. (°C)	Uv, ν_{max} (log ε) (in CH_2Cl_2)	IR, cm^{-1} (KBr pellet)	PMR (δ) (in $CDCl_3$)
I	(H-MP)Re(CO)$_3$	175-177	388 nm (Soret) 480 580	1740 (ester,CO) 1880 (νM-CO) 2020 " 3380 (νN-H)	10.5 (s), =CH- 10.2 (s) " 4.7-3.0 (m), alkyl 2.0-1.6 (t) " -4.9 (s), NH
II	(H-TPP)Re(CO)$_3$	302-304	402 nm (6.12) 473 (5.62) 670 (4.92)	1875 (νM-CO) 2010 " 3350 (νN-H)	9.13 (q), pyrrole 8.88 (d) " 8.72 (s) " 8.30 (m), phenyl 7.87 (m) " -4.00 (s), NH
III	MP[Re(CO)$_3$]$_2$	246-248	400 nm (Soret) 480 sh. 520	1730 (ester,CO) 1900 (νM-CO) 2015 "	10.30 (s), =CH- 4.7-3.0 (m), alkyl 2.0-1.6 (t) "
IV	TPP[Re(CO)$_3$]$_2$	350,dec.	408 nm (Soret) 485 sh 513	1900 (νM-CO) 2025 "	9.20 (s), pyrrole 8.30 (m), phenyl 7.80 (m) "
V	(OC)$_3$ReMPTc(CO)$_3$	238-240	398 nm (5.04) 480 sh (3.80) 513 (4.46)	1720 (ester, CO) 1740 " 1925 (νM-CO) 2030 " 2045 "	10.60 (s), =CH- 4.7-3.0 (m), alkyl 2.0-1.5 (m), alkyl
VI	(H-MP)Tc(CO)$_3$	181-182	388 nm (4.17) 473 (3.70) 580 (3.17)	1735 (ester, CO) 1900 (νM-CO) 1920 " 2025 " 3380 (νN-H)	10.5 (s), =CH- 10.2 (s) " 4.7-3.0 (m), alkyl 2.0-1.6 (t) " -4.90 (s), NH
VII	MP[Tc(CO)$_3$]$_2$	227-229	396 nm (4.43) 480 sh (3.60) 507 (3.93)	1740 (ester,CO) 1925 (νM-CO) 2036 "	10.40 (s), =CH- 4.7-3.0 (m), alkyl 2.0-1.7 (t) "

Table 1. Spectral data for unusual metalloporphyrin complexes. I-IX. (cont.)

VIII	TPP[$Tc(CO)_3]_2$	323-325	403 nm (Soret) 475 sh 504 670	1915 (νM-CO) 2030 "	
IX	Unknown derivative of VII.	260,dec.	358 nm 397 (Soret) 500 540	1725 (ester,CO) 1925 (νM-CO) 2044 "	

Table 2. Relative intensities of ion species of interest in the mass spectra of complexes I and III.

Ion Species	Relative Intensities	
	$(H\text{-}MP)Re(CO)_3$	$MP[Re(CO)_3]_2$
$(M)^+$	8.8	43.80
$(M\text{-}H)^+$	0.54	0.60
$(M\text{-}2H)^+$	0.08	0.20
$(M\text{-}CH_3O)^+$	1.80	4.00
$(M\text{-}2CO)^+$	0.25	5.30
$(M\text{-}CH_3CO_2)^+$	0.43	1.30
$(M\text{-}3CO)^+$	100.00	-
$(M\text{-}3CO\text{-}H)^+$	1.20	-
$(M\text{-}5CO)^+$	-	100.00
$(M\text{-}5CO\text{-}H)^+$	-	1.40
$(M\text{-}6CO)^+$	-	62.90
$(M\text{-}6CO\text{-}H)^+$	-	1.50
$(M)^{++}$	-	2.50
$(M\text{-}3CO)^{++}$	27.20	-
$(M\text{-}4CO)^{++}$	-	47.60

Isotope Peaks of parent ion	Relative Intensities	
	$(H\text{-}MP)Re(CO)_3$	$MP[Re(CO)_3]_2$
M	1.00	1.00
M + 1	0.50	0.59
M + 2	1.79	3.60
M + 3	0.77	1.71
M + 4	-	3.26
M + 5	-	1.38

Table 3. Visible Absorptions for (H-MP)$Re(CO)_3$, (I), and its Unstable Derivatives.

Derivatives	λ max (in acetone), nm.
(H-MP)$Re(CO)_3$, (I)	400 (Soret); 480, 580
(I) + CH_3COOAg	387 ("); 480, 560, 580
(I) + $(CH_3COO)_2Hg$	385 ("); 480, 530, 570, 580
(I) + $(CH_3COO)_2Pb \cdot 3H_2O$	388 ("); 460, 580
(I) + $(CH_3COO)_2Cu \cdot H_2O$	395 ("); 520, 560*

*This is the visible absorptions of Cu^{II} MPIXDME.

Crystal Data and Experimental Conditions

	$TPP[Re(CO)_3]_2$	$TPP[Tc(CO)_3]_2$
a	11.887(2) Å	11.934(1) Å
b	16.363(2) Å	16.295(1) Å
c	11.586(2) Å	11.596(1) Å
β	117.02°(1)°	117.02(1)°
Volume	2008 $Å^3$	2009 $Å^3$
Room Temperature	21°C	18°C
D_{calc}	1.908 g/cm^3	1.619 g/cm^3
D_{meas}	1.90 g/cm^3	1.61 g/cm^3
Mol. Wt.	1153.2 daltons ($C_{50}H_{28}O_6N_4Re_2$)	978.8 daltons ($C_{50}H_{28}O_6N_4Tc_2$)
Z	2	2
Space Group	$P2_1/c$	$P2_1/c$
μ(MoKα radiation)	64.4 cm^{-1}	7.37 cm^{-1}
Systematic Absences	h0l(l odd); 0k0(k odd)	Same
Scan Rate	1°/min. if peak height ≥ 3 cps 2°/min. if peak height < 3 cps	4°/min if 2θ ≤ 30° 2°/min if 2θ > 30°
Scan Range	1.50°	2.25°
Max sin θ/λ	0.65(27.5 in θ)	0.703(30° in θ)
Total Refln	4769	6013
Refln with $I \geq 3\sigma_I$	2385	3762
Coincidence Factor, τ	4.31 x 10^{-7} $counts^{-1}$	5.50 x 10^{-7} $counts^{-1}$
Stability Constant K	0.03	0.015
$R = \Sigma\|\|F_o\|-\|F_c\|\|/\Sigma\|F_o\|$	0.045	0.032
$R_w = \Sigma w\|\|F_o\|-\|F_c\|\|^2/\Sigma wF_o^2)^{1/2}$	0.044	0.027
$S.E.F. = (\Sigma w\|\|F_o\|-\|F_c\|\|^2/N_{obs}-N_{var})^{1/2}$	1.33	1.37

TABLE 5

Fractional Coordinates and Thermal Motion Parameters Derived from the Least Squares Refinement* for $TPP[Tc(CO)_3]_2$

*In this and subsequent tables estimated standard deviations for the least significant figure are in parentheses. The Debye-Waller factor is defined as:

$$T = \exp[-2\pi^2 \Sigma_i \Sigma_j a_i a_j h_i h_j U_{ij}]$$

The values for U have been multiplied by 10^4. Isotropic B's for hydrogen atoms defined by:

$$\exp[-B(\sin^2\theta)/\gamma^2]$$

are given in the column labeled U_{11}. These have been multiplied by 10.

ATOM	X	Y	Z	U(11)	U(22)	U(33)	U(12)	U(13)	U(23)
TC	-0.0901(1)	0.0515(1)	0.0342(1)	301(1)	238(1)	270(1)	7(1)	156(0)	19(1)
N(1)	-0.0644(2)	-0.0656(1)	0.1304(2)	292(12)	270(13)	238(10)	-23(10)	131(9)	-3(9)
N(2)	0.1345(2)	0.0425(1)	0.1422(2)	294(12)	281(13)	222(10)	-33(10)	110(9)	8(10)
C(1)	-0.1464(2)	-0.1293(1)	0.0877(2)	269(14)	282(14)	289(13)	-22(11)	145(12)	16(11)
C(2)	-0.1234(2)	-0.1837(1)	0.1943(2)	350(17)	298(16)	332(15)	-37(13)	170(13)	40(12)
C(3)	-0.0260(3)	-0.1523(2)	0.2988(3)	336(16)	359(16)	290(15)	10(14)	132(13)	82(13)
C(4)	0.0142(2)	-0.0796(1)	0.2578(2)	301(15)	302(14)	261(13)	8(12)	137(12)	25(11)
C(5)	0.1226(2)	-0.0340(1)	0.3278(2)	304(15)	313(16)	230(12)	14(11)	113(11)	18(11)
C(6)	0.1[illegible]4(2)	0.0195(1)	0.2735(2)	290(15)	368(15)	244(13)	-45(12)	115(12)	-18(12)
C(7)	0.2917(3)	0.0603(2)	0.3509(2)	393(17)	598(23)	230(13)	-195(18)	79(13)	-21(16)
C(8)	0.3207(3)	0.1082(2)	0.2745(3)	340(18)	577(23)	289(15)	-196(17)	78(14)	-21(15)
C(9)	0.2253(2)	0.0993(1)	0.1452(2)	302(16)	334(16)	289(14)	-73(13)	127(12)	-32(12)
C(10)	0.2300(2)	0.1412(1)	0.0421(2)	301(15)	275(14)	283(13)	-53(12)	137(12)	-4(11)
C(11)	0.1914(2)	-0.0[illegible]73(2)	0.4713(2)	285(13)	384(15)	225(12)	-53(15)	109(10)	22(13)
C(12)	0.2651(3)	-0.1159(2)	0.5221(3)	440(20)	527(22)	322(17)	88(17)	187(15)	33(16)
C(13)	0.3327(3)	-0.1270(2)	0.6547(3)	439(22)	683(27)	415(20)	203(20)	180(17)	208(19)
C(14)	0.3245(3)	-0.0693(2)	0.7363(3)	446(20)	855(33)	253(15)	53(20)	143(15)	125(18)
C(15)	0.2486(3)	-0.0024(2)	0.6880(3)	600(25)	629(26)	290(17)	12(20)	201(17)	-55(17)
C(16)	0.1812(3)	0.0086(2)	0.5549(3)	509(22)	451(20)	317(16)	61(17)	159(16)	15(15)
C(17)	0.3318(2)	0.2038(1)	0.0716(2)	301(15)	343(16)	267(14)	-70(13)	108(12)	13(12)
C(18)	0.4160(3)	0.1936(2)	0.0204(3)	373(17)	394(17)	363(17)	-35(15)	190(14)	-1(15)
C(19)	0.5105(3)	0.2504(2)	0.0469(3)	320(18)	578(24)	481(20)	-72(17)	186(16)	69(18)
C(20)	0.5219(3)	0.3172(2)	0.1222(3)	340(19)	477(22)	510(21)	-147(17)	116(17)	41(17)
C(21)	0.4378(3)	0.3290(2)	0.1711(3)	509(22)	360(20)	506(21)	-130(17)	181(18)	-88(16)
C(22)	0.3434(3)	0.2726(2)	0.1453(3)	407(20)	457(21)	453(20)	-109(16)	232(17)	-96(16)
C(23)	-0.1080(3)	0.1523(2)	-0.0568(3)	507(21)	379(18)	543(21)	50(16)	335(18)	71(16)
C(24)	-0.2652(2)	0.0557(2)	-0.0249(2)	383(17)	410(17)	302(14)	65(17)	163(13)	30(15)
C(25)	-0.0697(3)	0.1138(2)	0.1793(3)	464(20)	298(16)	543(20)	-43(15)	312(17)	-63(15)
O(1)	-0.1236(3)	0.2137(1)	-0.1099(3)	1080(26)	458(17)	1072(24)	263(17)	734(22)	374(17)
O(2)	-0.3711(2)	0.0604(1)	-0.1570(2)	336(13)	916(22)	569(15)	121(15)	178(11)	57(16)
O(3)	-0.0576(2)	0.1511(1)	0.2682(2)	909(23)	598(18)	737(19)	-149(16)	502(18)	-326(15)
H(1)	-0.165 (3)	-0.233 (1)	0.186 (2)	29(7)					
H(2)	0.037 (3)	-0.175 (2)	0.374 (3)	34(8)					
H(3)	0.335 (2)	0.055 (2)	0.434 (3)	32(6)					
H(4)	0.389 (2)	0.138 (1)	0.298 (2)	25(6)					
H(5)	0.268 (3)	-0.149 (2)	0.471 (3)	33(8)					
H(6)	0.382 (3)	-0.177 (2)	0.691 (3)	38(7)					
H(7)	0.366 (3)	-0.078 (1)	0.820 (3)	36(7)					
H(8)	0.245 (3)	0.034 (2)	0.738 (3)	41(9)					
H(9)	0.135 (2)	0.056 (2)	0.522 (2)	33(7)					
H(10)	0.415 (3)	0.145 (2)	-0.022 (3)	39(8)					
H(11)	0.563 (3)	0.238 (2)	0.016 (3)	45(10)					
H(12)	0.583 (3)	0.353 (2)	0.137 (3)	47(9)					
H(13)	0.438 (2)	0.373 (2)	0.210 (2)	26(7)					
H(14)	0.295 (3)	0.280 (2)	0.182 (3)	34(8)					

Table 5

TABLE 6

Fractional Coordinates and Thermal Motion Parameters Derived from the Least Squares Refinement for $TPP[Re(CO)_3]_2$*

*See footnote for Table 6. Hydrogen atom positions were assumed to be in their theoretically calculated positions. They are not listed here.

ATOM	X	Y	Z	U(11)	U(22)	U(33)	U(12)	U(13)	U(23)
RE	-0.0910(1)	0.0515(1)	0.0351(1)	344(2)	299(2)	313(2)	8(3)	169(1)	22(3)
N(1)	-0.0645(9)	-0.0657(5)	0.1314(9)	410(57)	264(58)	270(48)	-38(45)	161(47)	41(45)
N(2)	0.1334(8)	0.0416(6)	0.1408(8)	309(53)	368(61)	281(51)	-143(50)	157(45)	-45(52)
C(1)	-0.1469(10)	-0.1307(7)	0.0889(11)	213(57)	353(69)	434(72)	43(53)	219(58)	59(59)
C(2)	-0.1226(11)	-0.1814(6)	0.1977(11)	405(74)	254(61)	335(69)	-44(56)	212(63)	75(53)
C(3)	-0.0234(10)	-0.1516(7)	0.3014(11)	356(72)	383(71)	372(72)	-7(60)	213(63)	5(62)
C(4)	0.0149(12)	-0.0796(7)	0.2604(11)	439(78)	481(80)	240(63)	-41(61)	227(62)	114(56)
C(5)	0.1215(10)	-0.0343(6)	0.3281(10)	322(65)	298(71)	212(56)	-5(51)	65(52)	33(48)
C(6)	0.1758(11)	0.0196(8)	0.2710(13)	352(75)	493(78)	471(82)	-15(63)	235(69)	-83(67)
C(7)	0.2897(11)	0.0596(9)	0.3482(11)	412(71)	584(86)	349(68)	-33(77)	168(60)	59(77)
C(8)	0.3181(12)	0.1070(7)	0.2704(11)	452(80)	520(81)	274(66)	-220(66)	191(63)	17(62)
C(9)	0.2250(11)	0.0990(7)	0.1432(10)	379(72)	393(70)	196(58)	10(58)	155(57)	-35(55)
C(10)	0.2313(10)	0.1406(6)	0.0416(10)	311(65)	260(63)	283(64)	62(54)	132(56)	1(54)
C(11)	0.1916(9)	-0.0457(8)	0.4712(10)	299(56)	516(71)	345(60)	-75(66)	191(50)	-47(71)
C(12)	0.2670(13)	-0.1160(8)	0.5245(13)	498.89)	522(84)	513(86)	144(71)	271(77)	-32(72)
C(13)	0.3318(13)	-0.1248(9)	0.6557(13)	537(96)	755(112)	357(83)	342(86)	186(78)	225(82)
C(14)	0.3243(14)	-0.0665(10)	0.7351(12)	645(101)	863(131)	337(79)	-129(93)	236(78)	94(86)
C(15)	0.2497(14)	-0.0023(9)	0.6891(12)	753(113)	699(105)	226(65)	105(87)	213(74)	-17(71)
C(16)	0.1828(13)	0.0089(8)	0.5564(13)	635(93)	410(75)	448(81)	86(69)	258(74)	31(68)
C(17)	0.3341(11)	0.2029(7)	0.0711(11)	356(71)	436(77)	303(69)	-143(60)	108(60)	-126(59)
C(18)	0.4175(12)	0.1936(7)	0.0218(12)	455(77)	400(65)	418(77)	-66(65)	284(66)	0(64)
C(19)	0.5125(12)	0.2508(9)	0.0473(13)	492(80)	576(88)	567(90)	-78(79)	383(76)	74(80)
C(20)	0.5221(13)	0.3169(8)	0.1244(14)	440(91)	515(86)	593(103)	-196(73)	143(83)	92(76)
C(21)	0.4376(13)	0.3278(8)	0.1697(13)	568(94)	377(75)	514(89)	-143(68)	276(79)	-130(68)
C(22)	0.3444(12)	0.2707(8)	0.1437(13)	485(84)	466(86)	579(90)	-141(70)	342(77)	-33(75)
C(23)	-0.1059(13)	0.1497(9)	-0.0530(14)	648(101)	554(96)	602(102)	165(85)	483(89)	-23(87)
C(24)	-0.2641(13)	0.0555(8)	-0.0223(11)	745(98)	344(67)	277(65)	145(90)	269(69)	24(74)
C(25)	-0.0687(13)	0.1120(10)	0.1785(16)	413(93)	697(111)	802(125)	-105(80)	343(95)	213(98)
O(1)	-0.1213(11)	0.2112(6)	-0.1077(12)	1098(103)	577(75)	1299(112)	259(71)	866(94)	345(76)
O(2)	-0.3718(9)	0.0595(7)	-0.0568(9)	4.5(60)	1075(92)	532(64)	264(73)	188(53)	119(74)
O(3)	-0.0564(11)	0.1516(7)	0.2678(10)	1011(94)	680(78)	764(83)	-101(71)	571(78)	-315(69)

Table 6

Root - Mean - Square Amplitudes of Vibration (in Å) Along Principal Axes of Thermal Ellipsoids

	$TPP[Re(CO)_3]_2$			$TPP[Tc(CO)_3]_2$		
	AXIS 1	AXIS 2	AXIS 3	AXIS 1	AXIS 2	AXIS 3
M	0.165(2)	0.176(2)	0.188(1)	0.148(1)	0.158(1)	0.176(1)
N(1)	0.14(3)	0.18(2)	0.21(2)	0.150(6)	0.160(4)	0.175(4)
N(2)	0.13(3)	0.16(2)	0.22(2)	0.147(5)	0.159(4)	0.183(5)
C(1)	0.11(5)	0.18(2)	0.22(2)	0.148(9)	0.171(3)	0.175(6)
C(2)	0.12(4)	0.19(2)	0.20(2)	0.152(8)	0.187(3)	0.196(7)
C(3)	0.17(4)	0.20(2)	0.20(1)	0.153(6)	0.185(5)	0.206(5)
C(4)	0.10(6)	0.21(2)	0.23(2)	0.155(7)	0.172(6)	0.178(4)
C(5)	0.14(2)	0.17(2)	0.20(3)	0.150(5)	0.175(6)	0.180(5)
C(6)	0.17(4)	0.20(2)	0.24(2)	0.156(4)	0.167(7)	0.198(4)
C(7)	0.18(3)	0.20(2)	0.25(2)	0.148(4)	0.181(9)	0.274(5)
C(8)	0.13(5)	0.18(2)	0.27(2)	0.148(6)	0.185(8)	0.268(5)
C(9)	0.13(4)	0.19(2)	0.20(2)	0.156(5)	0.173(7)	0.198(5)
C(10)	0.15(3)	0.17(2)	0.19(2)	0.151(7)	0.168(5)	0.186(5)
C(11)	0.15(4)	0.18(2)	0.23(2)	0.147(6)	0.161(5)	0.206(5)
C(12)	0.17(4)	0.23(2)	0.26(2)	0.174(7)	0.197(6)	0.242(5)
C(13)	0.15(3)	0.21(4)	0.32(2)	0.165(6)	0.213(10)	0.287(5)
C(14)	0.16(4)	0.24(2)	0.31(2)	0.150(6)	0.216(7)	0.297(6)
C(15)	0.14(3)	0.25(2)	0.30(2)	0.161(7)	0.245(6)	0.257(6)
C(16)	0.20(2)	0.21(3)	0.26(2)	0.178(5)	0.205(6)	0.240(6)
C(17)	0.14(2)	0.20(4)	0.23(2)	0.157(6)	0.163(4)	0.206(6)
C(18)	0.16(5)	0.20(2)	0.23(2)	0.177(10)	0.192(4)	0.205(5)
C(19)	0.14(6)	0.25(2)	0.25(2)	0.164(9)	0.212(5)	0.256(6)
C(20)	0.16(4)	0.22(2)	0.30(3)	0.156(8)	0.214(5)	0.267(7)
C(21)	0.17(2)	0.22(4)	0.26(2)	0.165(6)	0.234(5)	0.247(8)
C(22)	0.16(5)	0.22(3)	0.26(3)	0.179(7)	0.195(9)	0.240(4)
C(23)	0.13(7)	0.24(2)	0.28(2)	0.184(10)	0.192(7)	0.248(4)
C(24)	0.15(4)	0.17(2)	0.28(2)	0.170(6)	0.182(7)	0.216(5)
C(25)	0.15(6)	0.25(2)	0.32(2)	0.168(5)	0.185(11)	0.242(3)
O(1)	0.21(2)	0.25(4)	0.40(1)	0.167(6)	0.256(10)	0.374(3)
O(2)	0.19(2)	0.24(2)	0.34(1)	0.176(4)	0.246(5)	0.307(4)
O(3)	0.18(4)	0.28(2)	0.34(1)	0.174(8)	0.269(7)	0.328(3)

TABLE 8

Bond Lengths (Å) in $TPP[Re(CO)_3]_2$ and $TPP[Tc(CO)_3]_2$ [a,b]

TYPE	$TPP[Re(CO)_3]_2$		$TPP[Tc(CO)_3]_2$	
M-N(1)	2.168(9)		2.161(2)	
M-N(2)	2.382(9)		2.393(2)	
M-N(2)'[c]	2.407(10)		2.414(2)	
M-C(23)	1.869(16)	1.855(13)	1.911(4)	1.892(17)
M-C(24)	1.854(16)		1.881(4)	
M-C(25)	1.847(19)		1.884(4)	
N(1)-C(1)	1.377(15)	1.377(1)	1.356(4)	1.359(4)
N(1)-C(4)	1.376(14)		1.362(3)	
C(1)-C(2)	1.424(18)	1.422(3)	1.444(5)	1.442(4)
C(3)-C(4)	1.420(20)		1.439(5)	
C(1)-C(10)'[c]	1.392(15)	1.380(17)	1.391(4)	1.390(2)
C(4)-C(5)	1.367(16)		1.389(4)	
C(2)-C(3)	1.336(14)		1.342(4)	
N(2)-C(6)	1.403(18)	1.416(17)	1.418(4)	1.416(3)
N(2)-C(9)	1.428(17)		1.414(5)	
C(6)-C(7)	1.400(17)	1.395(7)	1.412(4)	1.416(5)
C(8)-C(9)	1.390(14)		1.419(4)	
C(5)-C(6)	1.422(21)	1.406(22)	1.400(5)	1.400(1)
C(9)-C(10)	1.391(19)		1.400(5)	
C(7)-C(8)	1.344(22)		1.339(6)	
C(5)-C(11)	1.490(15)	1.499(12)	1.500(4)	1.501(1)
C(10)-C(17)	1.507(17)		1.502(4)	
C(11)-C(12)	1.416(18)	1.367(26)	1.375(5)	1.377(9)
C(11)-C(16)	1.370(21)		1.378(5)	
C(12)-C(13)	1.364(20)		1.386(5)	
C(13)-C(14)	1.355(24)		1.369(6)	
C(14)-C(15)	1.320(22)		1.363(6)	
C(15)-C(16)	1.385(18)		1.390(5)	
C(17)-C(18)	1.359(24)		1.389(6)	
C(17)-C(22)	1.363(19)		1.378(5)	
C(18)-C(19)	1.391(20)		1.381(6)	
C(19)-C(20)	1.374(22)		1.362(6)	

TABLE 8 (CONTINUED)

C(20)-C(21)	1.339(26)			1.373(7)	
C(21)-C(22)	1.373(20)			1.377(6)	
C(23)-O(1)	1.158(20)			1.144(5)	
C(24)-O(2)	1.156(19)	1.162(9)		1.147(4)	1.146(2)
C(25)-O(3)	1.172(23)			1.147(5)	
M-M'	3.126(1)			3.101(1)	
M-N(1)'[c]	3.230(3)			3.208(3)	
Ct[d]-N(1)	2.263(12)			2.253(3)	
Ct-N(2)	1.814(16)			1.836(4)	
Ct-C(1)	3.212(14)			3.183(4)	
Ct-C(4)	3.216(14)	3.214(3)		3.191(4)	3.189(8)
Ct-C(6)	2.892(12)			2.922(3)	
Ct-C(9)	2.914(12)	2.903(15)		2.927(3)	2.924(4)
Ct-C(5)	3.444(12)			3.441(4)	
Ct-C(10)	3.446(12)	3.445(1)		3.443(4)	3.442(1)
N(1)-N(2)	2.898(15)			2.909(4)	
N(1)-N(2)'[c]	2.903(14)	2.900(4)		2.904(3)	2.907(4)

a. Some nonbonding distances of interest are also given.

b. For averaged values, the figures in parentheses are the r.m.s. standard deviations.

c. Primed atoms related to unprimed by the symmetry operation x'=-x, y'=-y, z'=-z.

d. Ct = center of porphyrin ring.

TABLE 9

Bond Angles (deg) in $TPP[Re(CO)_3]_2$ and $TPP[Tc(CO)_3]_2$[a]

Angle	$TPP[Re(CO)_3]_2$		$TPP[Tc(CO)_3]_2$	
N(1)-M-N(2)	79.0(4)		79.2(1)	
N(1)-M-N(2)'[b]	78.6(4)		78.6(1)	
N(1)-M-C(23)	175.7(7)		176.5(2)	
N(1)-M-C(24)	95.4(5)		95.4(1)	
N(1)-M-C(25)	94.8(6)		94.8(1)	
N(2)-M-N(2)'[b]	98.5(4)		99.6(1)	
N(2)-M-C(23)	98.3(5)		99.2(2)	
N(2)-M-C(24)	171.1(5)		171.0(1)	
N(2)-M-C(25)	84.5(5)		84.6(1)	
N(2)'[b]-M-C(23)	98.6(6)		98.7(1)	
N(2)'[b]-M-C(24)	87.0(5)		86.3(1)	
N(2)'[b]-M-C(25)	172.0(7)		171.3(2)	
C(23)-M-C(24)	87.6(7)		86.6(2)	
C(23)-M-C(25)	88.3(8)		88.0(2)	
C(24)-M-C(25)	89.2(6)		88.6(2)	
M-N(1)-C(1)	125.9(7)		125.3(2)	
M-N(1)-C(4)	124.9(8)		125.0(2)	
C(1)-N(1)-C(4)	106.6(10)		107.2(2)	
M-N(2)-C(6)	110.0(9)		110.5(2)	
M-N(2)-C(9)	129.1(7)		129.6(2)	
C(6)-N(2)-C(9)	104.5(9)		104.3(2)	
M-N(2)'[b]-C(6)'[b]	125.7(8)		125.1(2)	
M-N(2)'[b]-C(9)'[b]	107.2(8)		107.9(2)	
N(1)-C(1)-C(2)	107.9(9)	108.7(11)	109.4(2)	109.3(2)
N(1)-C(4)-C(3)	109.5(10)		109.1(2)	

TABLE 9 (CONTINUED)

N(1)-C(1)-C(10)'[b]	121.5(12)	121.9(5)	123.1(3)	123.0(1)
N(1)-C(4)-C(5)	122.2(12)		123.0(3)	
C(2)-C(1)-C(10)'[b]	130.5(11)	129.1(20)	127.2(3)	127.4(2)
C(3)-C(4)-C(5)	127.7(10)		127.5(3)	
C(1)-C(2)-C(3)	108.9(11)	107.9(15)	106.7(3)	107.0(4)
C(2)-C(3)-C(4)	106.8(11)		107.3(3)	
N(2)-C(6)-C(7)	109.8(13)	109.1(10)	109.4(3)	109.3(1)
N(2)-C(9)-C(8)	108.4(11)		109.3(3)	
N(2)-C(6)-C(5)	129.9(10)	129.8(2)	129.3(2)	129.0(4)
N(2)-C(9)-C(10)	129.7(9)		128.7(2)	
C(5)-C(6)-C(7)	120.3(12)	121.1(11)	121.4(3)	121.7(4)
C(8)-C(9)-C(10)	121.9(12)		121.9(3)	
C(6)-C(7)-C(8)	107.8(11)	108.7(12)	108.6(3)	108.5(2)
C(7)-C(8)-C(9)	109.6(12)		108.3(3)	
C(4)-C(5)-C(6)	124.6(11)	124.8(3)	124.8(3)	124.7(1)
C(9)-C(10)-C(1)'[b]	125.0(11)		124.6(3)	
C(4)-C(5)-C(11)	118.4(12)	117.6(16)	117.8(3)	117.6(8)
C(6)-C(5)-C(11)	116.9(10)		117.2(3)	
C(1)'[b]-C(10)-C(17)	115.7(12)		116.8(3)	
C(9)-C(10)-C(47)	119.3(9)		118.6(2)	
C(5)-C(11)-C(12)	120.7(12)	121.2(10)	120.8(3)	120.7(13)
C(5)-C(11)-C(16)	122.2(11)		120.5(3)	
C(10)-C(17)-C(18)	120.0(11)		120.4(3)	
C(10)-C(17)-C(22)	121.8(14)		119.2(3)	

TABLE 9 (CONTINUED)

C(12)-C(11)-C(16)	117.1(11)		118.7(3)	
C(11)-C(12)-C(13)	119.8(14)		121.1(4)	
C(12)-C(13)-C(14)	120.3(14)		119.3(4)	
C(13)-C(14)-C(15)	121.6(12)		120.5(4)	
C(14)-C(15)-C(16)	119.7(15)		120.0(4)	
C(15)-C(16)-C(11)	121.3(13)		120.4(3)	
C(18)-C(17)-C(22)	118.2(13)	120.0(13)	118.4(3)	120.0(9)
C(17)-C(18)-C(19)	120.8(13)		120.0(3)	
C(18)-C(19)-C(20)	119.1(16)		120.7(4)	
C(19)-C(20)-C(21)	120.3(14)		119.9(4)	
C(20)-C(21)-C(22)	119.8(14)		119.8(4)	
C(21)-C(22)-C(17)	121.7(16)		121.2(4)	
M-C(23)-O(1)	176.3(16)		176.6(4)	
M-C(24)-O(2)	178.6(13)	177.8(13)	177.3(3)	177.7(13)
M-C(25)-O(3)	178.5(13)		179.3(4)	

a. For averaged values, the figures in parentheses are the r.m.s. standard deviations.

b. Primed atoms related to unprimed by the symmetry operation x' = -x, y' = -y, z' = -z

TABLE 10

A. Deviation (Å) from Least-Squares Planes for $TPP[Re(CO)_3]_2$ and $TPP[Tc(CO)_3]_2$

	Plane 1 (4 pyrrole N)		Plane 2 (pyrrole 1)		Plane 3 (pyrrole 2)	
	Re	Tc	Re	Tc	Re	Tc
M	-1.429	-1.419	0.666	0.647	1.326	1.314
N(1)	0.0	0.0	0.024	0.022	0.133	0.139
N(2)	0.0	0.0	-0.896	-0.904	-0.011	-0.007
C(1)	0.379	0.360	-0.024	-0.013	-0.240	-0.216
C(2)	0.891	0.917	0.016	-0.001	-0.538	-0.552
C(3)	0.909	0.904	-0.001	0.013	-0.438	-0.418
C(4)	0.369	0.373	-0.015	-0.022	-0.036	-0.030
C(5)	0.345	0.357	-0.206	-0.219	0.028	0.031
C(6)	0.204	0.221	-0.639	-0.652	0.009	0.006
C(7)	0.275	0.288	-0.885	-0.900	-0.004	-0.003
C(8)	0.093	0.103	-1.261	-1.275	-0.003	-0.002
C(9)	-0.094	-0.089	-1.268	-1.278	0.004	0.006
C(10)	-0.289	-0.294	-1.636	-1.645	-0.006	-0.008
N(1)'[a]	0.0	0.0	-1.817	-1.828	-	-
N(2)'[a]	0.0	0.0	-	-	-0.330	-0.339

a. Primed atoms related to unprimed by center of symmetry.

TABLE 10 (Continued)

B. INTERPLANAR ANGLES (in deg)

Plane	1		2		3		4	
	Re	Tc	Re	Tc	Re	Tc	Re	Tc
2	24.0	24.2	—	—				
3	9.2	9.5	17.0	17.0	—	—		
4	82.5	82.8	63.7	63.9	79.5	79.6	—	—
5	54.6	54.3	72.6	72.6	63.7	63.6	88.5	88.2

Plane 1: 4 Pyrrole nitrogen atoms

Re: $7.198x - 13.017y - 2.972z = 0.0$

Tc: $7.223x - 12.966y - 2.954z = 0.0$

Plane 2: Pyrrole Ring 1 [N(1), C(1) - C(4)]

Re: $-9.696x + 8.726y + 6.606z = 0.8962$

Tc: $-9.751x + 8.650y + 6.628z = 0.9032$

Plane 3: Pyrrole Ring 2 [N(2), C(6) - C(9)]

Re: $-7.645x + 12.347y + 4.727z = 0.1702$

Tc: $-7.689x + 12.272y + 4.768z = 0.1731$

Plane 4: Phenyl Ring [C(11) - C(16)]

Re: $10.317x + 8.127y - 4.536z = -0.5543$

Tc: $10.328x + 8.165y - 4.527z = -0.5606$

Plane 5: Phenyl Ring 2 [C(17) - C(22)]

Re: $3.065x - 8.340y + 7.115z = -0.1750$

Tc: $3.084x - 8.368y + 7.091z = -0.1857$

Note: All planes are unweighted. x,y,z are in monoclinic fractional coordinates.